Supplementary figures and material and methods

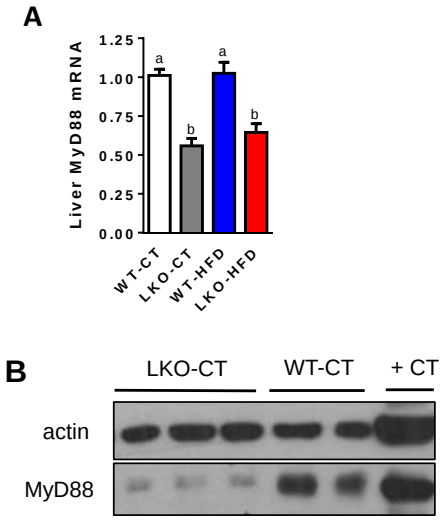

Figure S1: Validation of hepatocyte MyD88 deletion

(**A**) mRNA expression of *Myd88* in the liver of LKO mice and WT under CT diet and HFD (n=31-40). Data are presented as the mean ± SEM. Data with different superscript letters are significantly different ($p < 0.05$) according to post-hoc ANOVA one-way statistical analysis. (**B**) Representative liver immunoblot of MyD88 and β-actin in WT mice and LKO mice. + CT, corresponds to positive control protein (uterus).

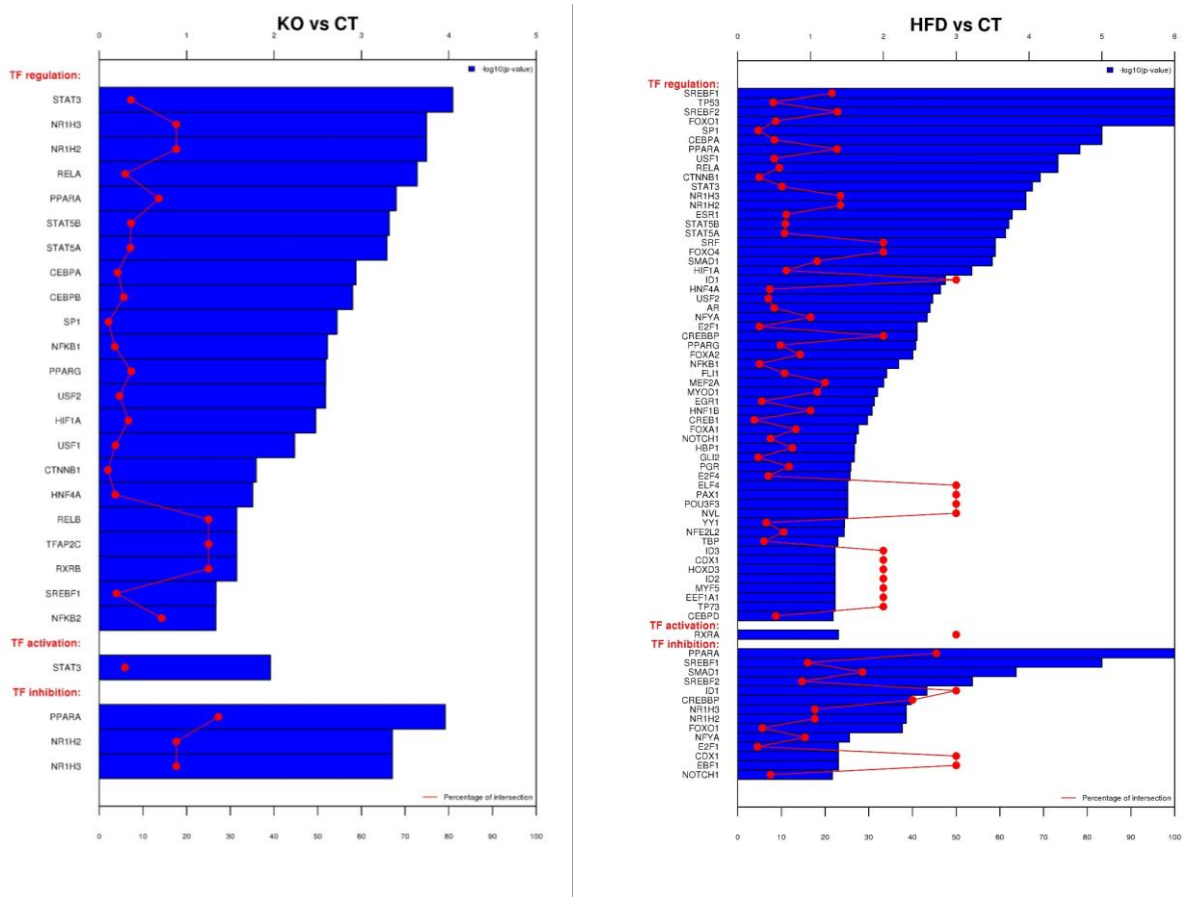

Figure S2: TFactS analysis of h**epatocyte *Myd88* deletion and HFD treated mice**

Transcription factor predictions by TFactS. The list of genes that were significantly modified in LKO-CT mice compared to WT-CT mice and WT-HFD compared to WT-CT was submitted to TFactS. The number of genes in the intersection between the submitted lists and the interrogated databases is presented as a percentage. The regulation type of transcription factors (activation or inhibition) is indicated if it was found significant ($p < 0.05$) by TFactS (sign-sensitive). Only transcription factors with a minimum of five target genes in the catalogue were considered.

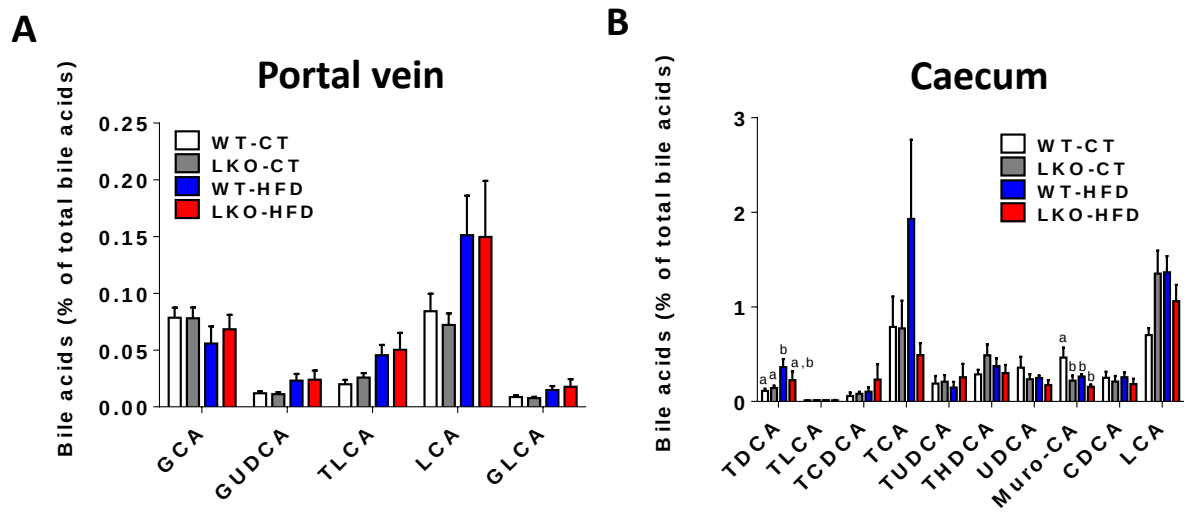

Figure S3: Hepatocyte *Myd88* deletion affects plasma bile acids profile

(**A**) Plasma bile acids (% of total bile acids), (**B**) Caecum bile acids. CA: cholic acid; UDCA: ursodeoxycholic acid; LCA: lithocholic acid; DCA: deoxycholic acid; CDCA: chenodeoxycholic acid; HDCA: hyodeoxycholic acid; Muro-CA: muricholic acid (T: taurine conjugated species; G: glycine conjugated species). Data are presented as the mean ± SEM (n=9-10). Data with different superscript letters or symbols are significantly different ($p < 0.05$) according to post-hoc one-way ANOVA.

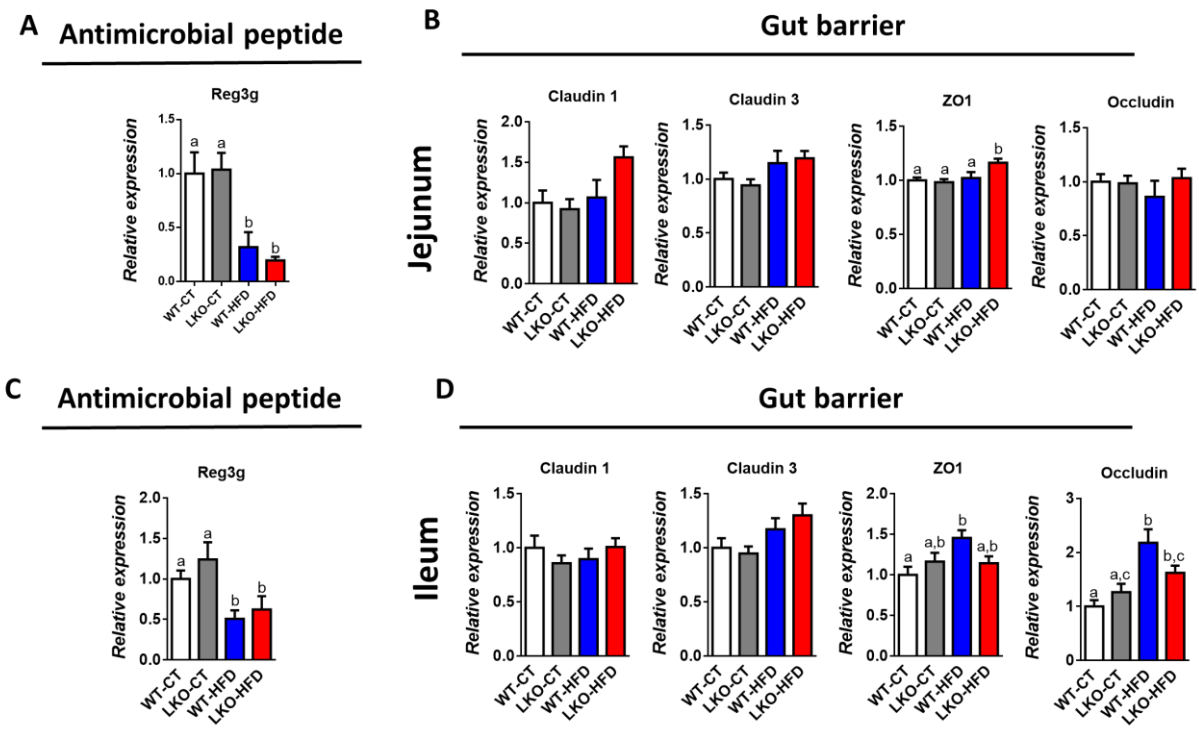

Figure S4: Markers of gut barrier function in the jejunum and in the ileum.

Antimicrobial peptide : Reg3g mRNA in the jejunum (**A**) and in the ileum (**C**). Markers of tight junction proteins (Claudin 1 and 3, ZO1 and occludin) in the jejunum (**B**) and in the ileum (**D**) of WT-CT, LKO-CT, WT-HFD and LKO-HFD mice. Data are presented as the mean ± SEM (n=10-12). Data with different superscript letters are significantly different ($p < 0.05$) according to post-hoc one-way ANOVA.

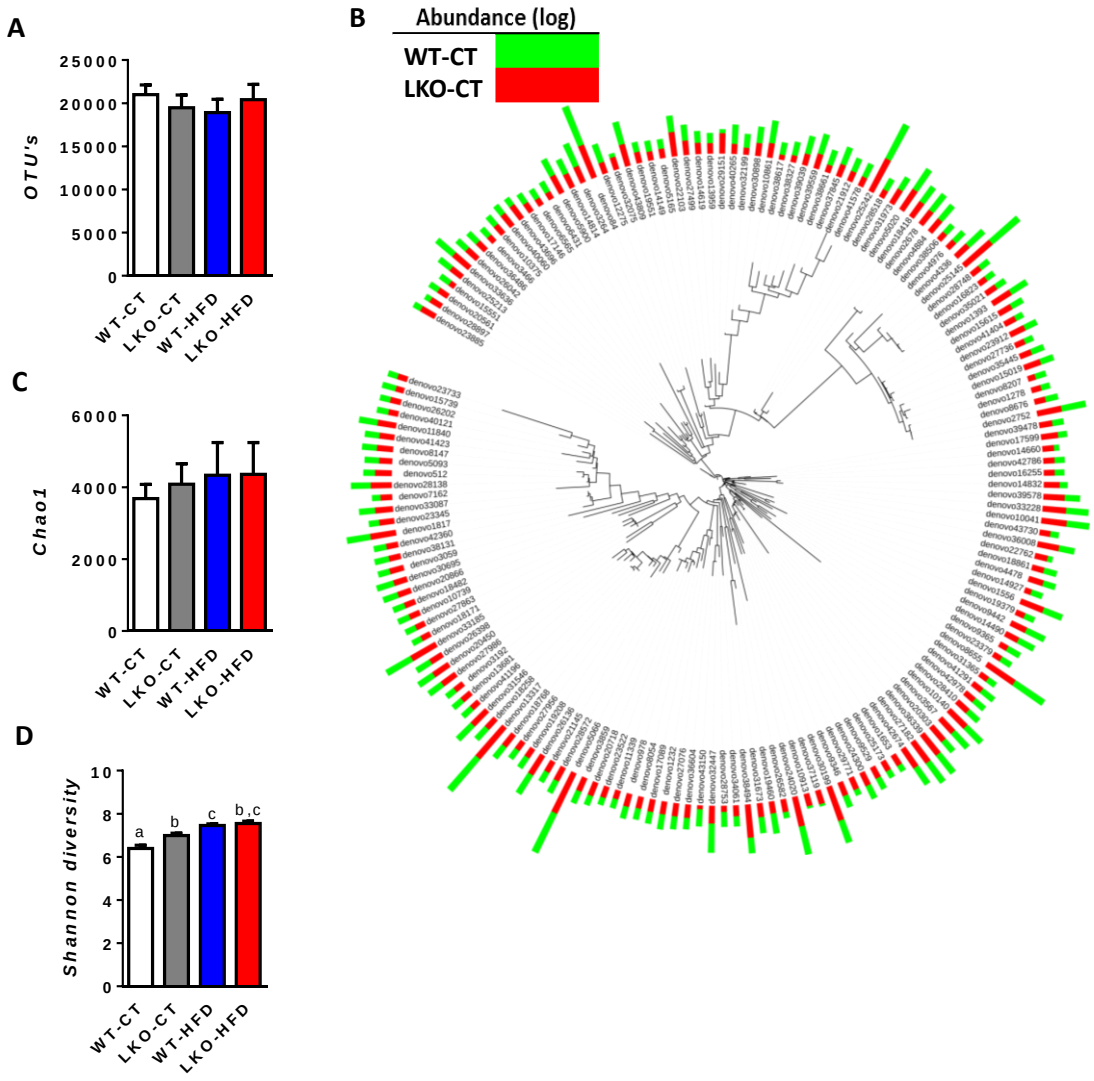

Figure S5: Gut microbiota markers of diversity and richness

(**A**) Mean number of operational taxonomic units (OTU's), (**B**) The tree was built with fasttree using representative sequences of OTUs as input. Only OTUs which contained more than 10 sequences (median number in all the samples from the STD group) were used. Abundance is represented as the log of the median number of sequences in the OTUs. The taxonomic identification of the 10 most abundant OTUs is given as indication. In brackets: highest level of taxonomic identification: p = phylum; f = family; g = genus. (**C**) Chao1 richness (**D**) Shannon diversity. Data are presented as the mean ± SEM (n=12). Data with different superscript letters are significantly different ($p < 0.05$) according to post-hoc one-way ANOVA.

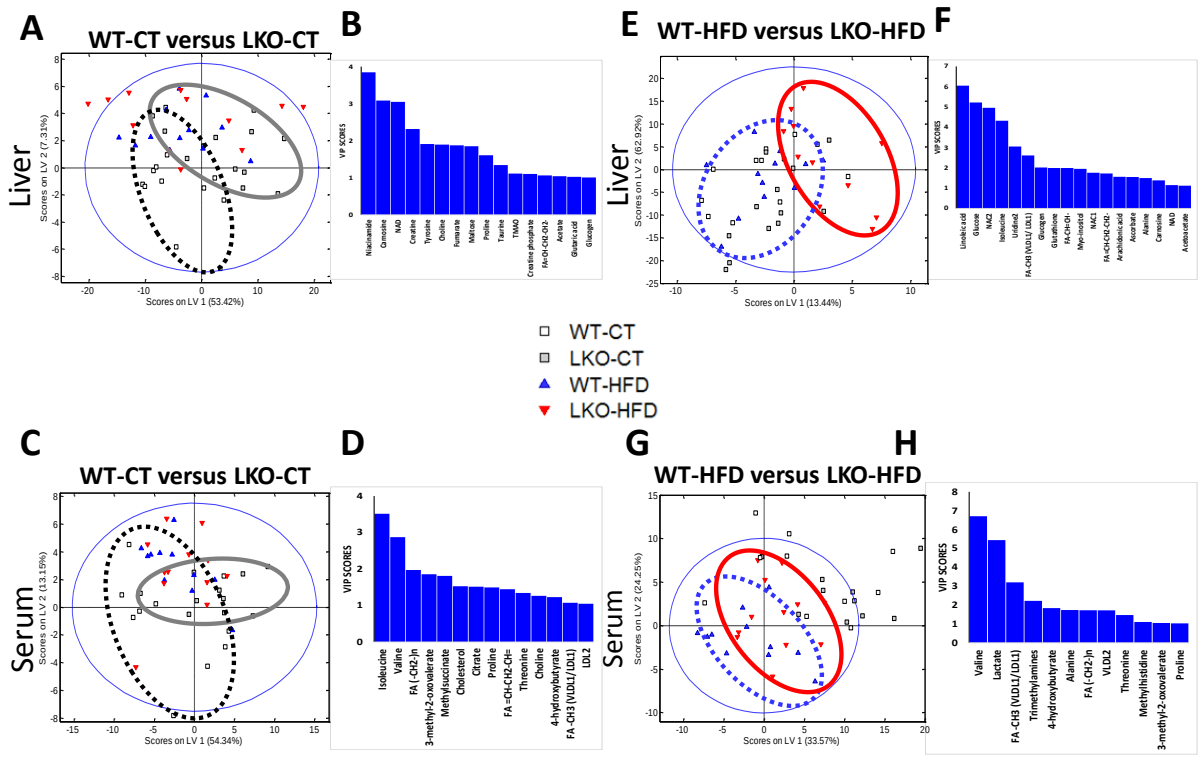

Figure S6. PLS DA analysis of the effect of deletion of MyD88 on the metabolome.

(**A-D**) PLS-DA scores plot and VIP scores for discrimination models based on liver metabolome (R2CV 0.115, RMSECV 0.743) (**A, B**) and serum metabolome (R2CV 0.104, RMSECV 0.723) **(C, D)** for discrimination between WT and LKO under CT treatment. Only samples from animals under CT treatment have been used to build the model. Samples from animals under HFD treatment (both WT and LKO) have been projected into the scores plot to seek for further metabolomic similarities.

(**E-F**) PLS-DA scores plot based and VIP scores for discrimination models based on liver metabolome (R2CV 0.198, RMSECV 0.755) **(E, F**) and the serum metabolome (R2CV 0.003, RMSECV 0.765) **(G, H)** for discrimination between WT and LKO under HFD treatment. Only samples from animals under HFD treatment have been used to build the model. Samples from animals under CT treatment (both WT and LKO) have been projected into the scores plot to seek for further metabolomic similarities.

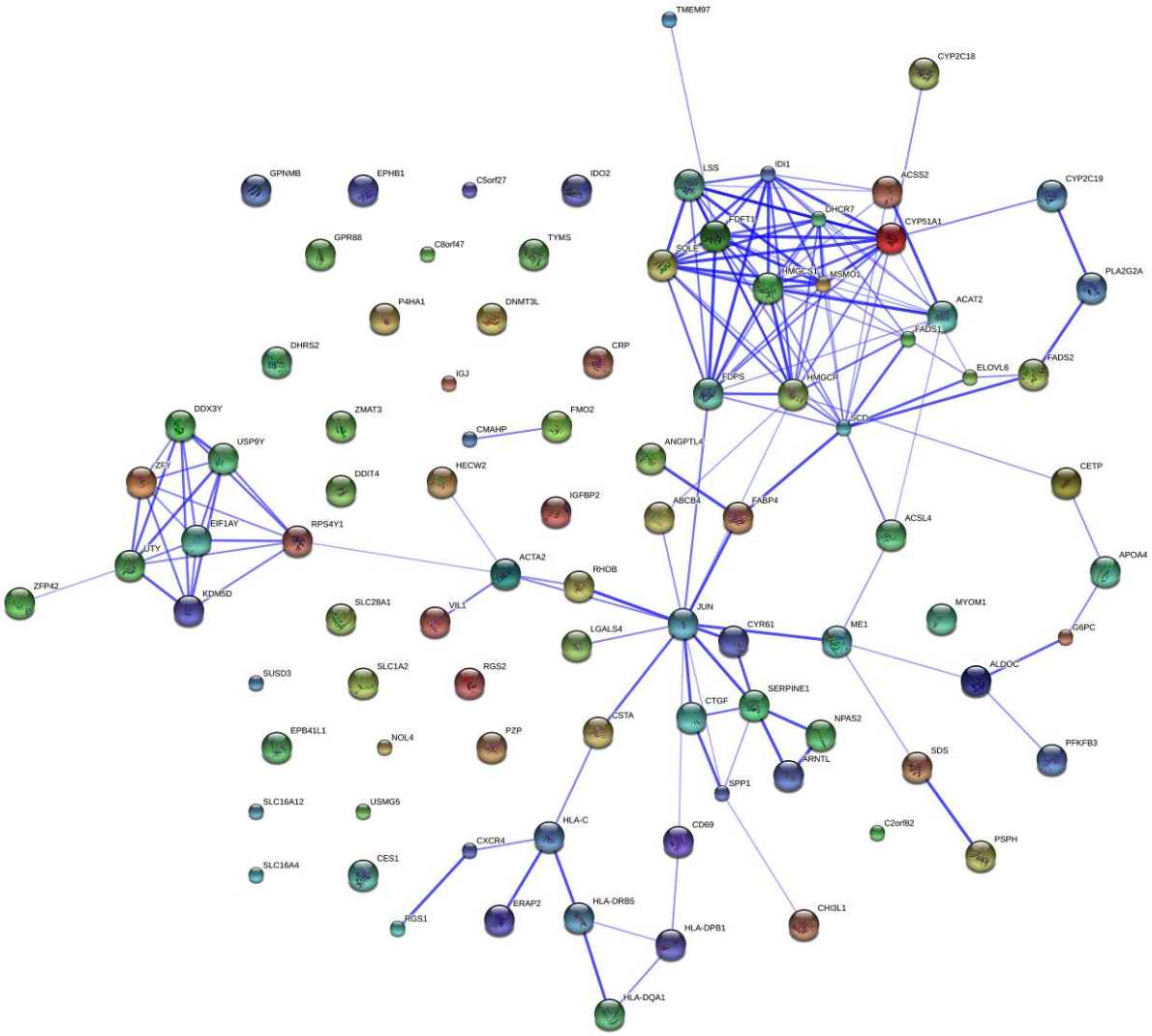

Figure S7 Graphic representation of the reported interactions between the differentially expressed genes between OBESE and NASH patients. All genes with a fold change greater than 2log +1 or below 2log -1 were loaded into the STRING 10 software. Predicted interactions are indicated with a blue line.

Documents with DAVID files are tables of biological processes affected in LKO-CT mice, WT-HFD mice and LKO-HFD mice compared to WT-CT mice. Biological processes similarly affected in LKO-CT mice and LKO-HFD mice, in LKO-CT mice and WT-HFD mice, in WT-HFD mice and LKO-HFD mice and biological processes similarly affected in LKO-CT, WT-HFD and LKO-HFD are also represented. These tables have been generated using the David web tool.

LKO

Term	Count	PValue	Genes
GO:0055114~oxidation reduction	33	2,17E-11	STEAP4, HTATIP2, CYP2J9, POLR2L, EHHADH, CYP2B9, AKR1C13, GPD1L, CBR1, CRYL1, HMOX1, FMO3, IDH2, CYP3A44, CYP2C55, SCD2, CYP3A16, CYP2D40, CYP3A11, DHRS9, CYP2B13, MOXD1, CYP4A10, CYP2A22, NDOR1, CYP7B1, CYP17A1, SQLE, AOX1, CYP4A31, CYP3A59, CYP2C38, RDH16, CYP4A14, CYP2A4
GO:0051186~cofactor metabolic process	13	2,21E-06	GSTA1, SLC11A2, CBR1, AK157302, HMOX1, EHHADH, PDK4, ACOT2, IDH2, ACOT1, ACOT4, PDSS2, ACOT3
GO:0006953~acute-phase response	6	2,77E-05	ORM1, SERPINA3N, SAA2, SAA1, SAA3, ORM2
GO:0006637~acyl-CoA metabolic process	5	8,73E-05	EHHADH, ACOT2, ACOT1, ACOT4, ACOT3
GO:0007586~digestion	5	2,54E-04	PNLIP, CYP7B1, CLPS, PNLIPRP2, CTRB1
GO:0006732~coenzyme metabolic process	9	3,54E-04	GSTA1, EHHADH, PDK4, IDH2, ACOT2, ACOT1, ACOT4, PDSS2, ACOT3
GO:0002526~acute inflammatory response	7	4,48E-04	ORM1, SERPINA3N, C4A, SAA2, SAA1, SAA3, ORM2
GO:0006952~defense response	14	0,003229938	CXCL1, ORM1, SERPINA3N, PNLIPRP2, C4A, SAA2, SAA1, GM15315, H2-Q1, SAA3, BCL3, CXCL11, ORM2, DEFA-RS12
GO:0034754~cellular hormone metabolic process	5	0,003607275	CYP17A1, RBP1, ESR1, DHRS9, RDH16
GO:0042445~hormone metabolic process	6	0,004762838	CYP17A1, RBP1, CHST8, ESR1, DHRS9, RDH16
GO:0016042~lipid catabolic process	7	0,005859988	PNLIP, CEL, CLPS, PNLIPRP1, PNLIPRP2, EHHADH, PLBD2
GO:0006954~inflammatory response	9	0,006216803	CXCL1, ORM1, SERPINA3N, C4A, SAA2, SAA1, SAA3, CXCL11, ORM2
GO:0006575~cellular amino acid derivative metabolic process	7	0,007466696	GSTA1, CHKA, OAZ1, CSAD, SLC22A5, FABP5, MOXD1
GO:0006775~fat-soluble vitamin metabolic process	4	0,007983589	CBR1, RBP1, DHRS9, RDH16
GO:0006766~vitamin metabolic process	5	0,009829245	CBR1, RBP1, DHRS9, SLC22A5, RDH16
GO:0006576~biogenic amine metabolic process	5	0,016237559	CHKA, OAZ1, SLC22A5, FABP5, MOXD1
GO:0042573~retinoic acid metabolic process	3	0,017685864	RBP1, DHRS9, RDH16
GO:0010817~regulation of hormone levels	6	0,019906047	CYP17A1, RBP1, CHST8, ESR1, DHRS9, RDH16
GO:0006720~isoprenoid metabolic process	4	0,021544477	RBP1, DHRS9, RDH16, PDSS2
GO:0008610~lipid biosynthetic process	9	0,023111047	CHKA, CYP7B1, CYP17A1, ISYNA1, SCD2, DHRS9, RDH16, FABP5, PDSS2
GO:0042092~T-helper 2 type immune response	2	0,024139564	BCL3, BCL6
GO:0032764~negative regulation of mast cell cytokine production	2	0,024139564	HMOX1, BCL6
GO:0007263~nitric oxide mediated signal transduction	2	0,024139564	MT2, MT1
GO:0006631~fatty acid metabolic process	7	0,024836662	CYP4A10, CRYL1, SCD2, POLR2L, EHHADH, CYP4A31, ACOT1, ACOT4, ACOT3
GO:0006955~immune response	12	0,028728031	CXCL1, CD8B1, C4A, GP49A, PRG4, H2-Q1, GBP10, BCL3, BCL6, H2-T10, SPON2, CXCL11
GO:0008299~isoprenoid biosynthetic process	3	0,028876807	DHRS9, RDH16, PDSS2
GO:0002719~negative regulation of cytokine production during immune response	2	0,035991247	HMOX1, BCL6
GO:0032763~regulation of mast cell cytokine production	2	0,035991247	HMOX1, BCL6
GO:0002701~negative regulation of production of molecular mediator of immune response	2	0,035991247	HMOX1, BCL6
GO:0010273~detoxification of copper ion	2	0,035991247	MT2, MT1
GO:0006776~vitamin A metabolic process	3	0,039369746	RBP1, DHRS9, RDH16
GO:0016101~diterpenoid metabolic process	3	0,045077825	RBP1, DHRS9, RDH16
GO:0001523~retinoid metabolic process	3	0,045077825	RBP1, DHRS9, RDH16
GO:0006508~proteolysis	20	0,04567435	CELA3B, ATG10, C4A, SOCS2, CTRB1, TRY4, UBE2H, KLK1, CELA1, MMP12, XRCC6BP1, CHST8, CPA2, 2210010C04RIK, GM5409, CELA2A, CPA1, CPB1, NFX1, CTRL
GO:0009636~response to toxin	3	0,048039489	CYP17A1, MT2, MT1
GO:0006721~terpenoid metabolic process	3	0,048039489	RBP1, DHRS9, RDH16
GO:0006869~lipid transport	5	0,05699611	APOL7E, PNLIP, CD36, ATP11A, PLTP
GO:0006826~iron ion transport	3	0,057329561	SLC11A2, STEAP4, GM5635
GO:0043627~response to estrogen stimulus	3	0,060554454	HMOX1, ARSA, ESR1
GO:0009611~response to wounding	9	0,0612289	CXCL1, ORM1, SERPINA3N, C4A, SAA2, SAA1, SAA3, CXCL11, ORM2
GO:0010876~lipid localization	5	0,070565265	APOL7E, PNLIP, CD36, ATP11A, PLTP
GO:0042905~9-cis-retinoic acid metabolic process	2	0,070694693	DHRS9, RDH16
GO:0042904~9-cis-retinoic acid biosynthetic process	2	0,070694693	DHRS9, RDH16
GO:0002467~germinal center formation	2	0,070694693	BCL3, BCL6
GO:0035238~vitamin A biosynthetic process	2	0,070694693	DHRS9, RDH16
GO:0016051~carbohydrate biosynthetic process	4	0,080057941	PGM3, ISYNA1, B3GALT1, CHST8
GO:0042362~fat-soluble vitamin biosynthetic process	2	0,081984296	DHRS9, RDH16
GO:0002718~regulation of cytokine production during immune response	2	0,081984296	HMOX1, BCL6
GO:0006882~cellular zinc ion homeostasis	2	0,081984296	MT2, MT1
GO:0046688~response to copper ion	2	0,081984296	MT2, MT1
GO:0006656~phosphatidylcholine biosynthetic process	2	0,081984296	CHKA, FABP5
GO:0055069~zinc ion homeostasis	2	0,093137568	MT2, MT1
GO:0019751~polyol metabolic process	3	0,095840049	GPD1L, ISYNA1, GPCPD1
GO:0051188~cofactor biosynthetic process	4	0,098868598	SLC11A2, AK157302, PDK4, PDSS2

WT-HFD

Term	Count	PValue	Genes
GO:0055114~oxidation reduction	64	6,91E-17	STEAP4, HTATIP2, CYP2J9, CYP2C68, EHHADH, HIBADH, RDH9, UQCR10, CYP39A1, HMOX1, SRD5A2, CYP3A44, CYP2C55, CYP2C54, CYP3A16, CYP3A11, CYP2B13, DHRS9, PPARGC1A, VAT1, MOXD1, COQ6, CYP4A32, ALDH1B1, SQLE, CYP4A31, CYP3A59, KDSR, STEAP2, G6PD2, PRODH, CYP2A4, NDUFB3, ME1, HSD3B3, CYP2B9, UGDH, GPD1L, CBR1, FMO3, FASN, HSD17B6, SCD1, CYP2D40, PYROXD2, CYP21A1, NDUFA7, IDO2, CYP4B1, CYP4A10, CYP7B1, NDOR1, DBT, CYP2A22, RDH11, CYP17A1, HSDL2, AKR1C19, AOX1, GM6444, DIO1, CYP4A14, RDH16, CYP2C38, CYP2C39, RETSAT
GO:0008202~steroid metabolic process	19	1,06E-06	SREBF1, OSBPL5, SOAT2, HSD3B3, LEPR, CYP21A1, HMGCS1, FDPS, PMVK, SIGMAR1, RDH9, CYP7B1, CYP17A1, CYP39A1, INSIG2, SULT1B1, SAA1, HSD17B6, SRD5A2
GO:0002526~acute inflammatory response	12	2,18E-05	C1RB, SERPINA3N, C4A, SAA2, SAA1, SAA3, SAA4, C2, CFD, FCGR1, ORM2, ORM3
GO:0008610~lipid biosynthetic process	23	3,23E-05	SCD1, HSD3B3, CHKA, CYP21A1, UGCG, HMGCS1, FDPS, DHRS9, ACACB, PMVK, SIGMAR1, PDSS2, RDH9, CYP7B1, CYP17A1, CYP39A1, INSIG2, ELOVL5, ELOVL3, FASN, SRD5A2, RDH16, FABP5
GO:0006694~steroid biosynthetic process	11	3,73E-05	HSD3B3, CYP7B1, CYP17A1, CYP39A1, INSIG2, CYP21A1, FDPS, HMGCS1, SRD5A2, PMVK, SIGMAR1
GO:0016125~sterol metabolic process	11	7,58E-05	SREBF1, SOAT2, CYP7B1, CYP39A1, INSIG2, SAA1, LEPR, FDPS, HMGCS1, PMVK, SIGMAR1
GO:0008203~cholesterol metabolic process	10	1,87E-04	SREBF1, SOAT2, CYP7B1, CYP39A1, INSIG2, SAA1, LEPR, FDPS, HMGCS1, PMVK
GO:0006953~acute-phase response	7	1,93E-04	SERPINA3N, SAA2, SAA1, SAA3, SAA4, ORM2, ORM3
GO:0006637~acyl-CoA metabolic process	6	2,21E-04	DBT, ACNAT2, EHHADH, ACOT2, ACOT1, ACOT3
GO:0008299~isoprenoid biosynthetic process	6	3,58E-04	RDH9, FDPS, HMGCS1, DHRS9, RDH16, PDSS2
GO:0006720~isoprenoid metabolic process	8	5,06E-04	RDH9, RDH11, FDPS, HMGCS1, DHRS9, RDH16, PDSS2, RETSAT
GO:0009611~response to wounding	23	5,48E-04	CXCL1, F11, C4A, PIK3CB, PPARG, MYH2, SAA3, SAA4, TLR5, CXCL11, MDK, FCGR1, SLC1A2, SERPINA3N, C1RB, SAA2, SAA1, CXCL13, C2, ID3, CFD, ORM2, ORM3
GO:0007586~digestion	6	8,13E-04	PNLIP, CYP7B1, CLPS, PNLIPRP2, CYP39A1, CTRB1
GO:0006575~cellular amino acid derivative metabolic process	13	8,59E-04	GSTA1, CHKA, OAZ1, CKM, GCLC, CSAD, CKMT2, IDO2, SLC22A5, TPMT, FABP5, MOXD1, AMD2
GO:0051186~cofactor metabolic process	15	9,00E-04	GSTA1, GCLC, EHHADH, ACNAT2, PDK4, ACOT2, ACOT1, ACSS2, HIBADH, PDSS2, ACOT3, COQ6, DBT, CBR1, HMOX1
GO:0006954~inflammatory response	17	9,30E-04	CXCL1, C4A, PPARG, SAA3, SAA4, TLR5, CXCL11, FCGR1, SERPINA3N, C1RB, SAA2, CXCL13, SAA1, C2, CFD, ORM2, ORM3
GO:0006732~coenzyme metabolic process	13	9,72E-04	GSTA1, DBT, GCLC, ACNAT2, EHHADH, PDK4, ACOT2, ACOT1, ACSS2, HIBADH, PDSS2, COQ6, ACOT3
GO:0010876~lipid localization	12	0,001289925	PNLIP, OSBPL5, SPNS2, CAV1, PLIN2, APOA5, PPARG, ATP11A, APOL9A, APOL9B, SIGMAR1, PLTP, SLCO2A1
GO:0006869~lipid transport	11	0,002496744	PNLIP, OSBPL5, SPNS2, PLIN2, APOA5, PPARG, ATP11A, APOL9A, APOL9B, SIGMAR1, PLTP, SLCO2A1
GO:0006775~fat-soluble vitamin metabolic process	6	0,002841622	RDH9, RDH11, CBR1, DHRS9, RDH16, RETSAT
GO:0006766~vitamin metabolic process	8	0,003863134	RDH9, RDH11, CBR1, GCLC, DHRS9, SLC22A5, RDH16, RETSAT
GO:0034754~cellular hormone metabolic process	7	0,003870622	RDH9, RDH11, CYP17A1, DHRS9, SRD5A2, RDH16, RETSAT
GO:0016042~lipid catabolic process	11	0,005835149	PNLIP, CEL, HACL1, CLPS, PNLIPRP1, PNLIPRP2, CYP39A1, ENPP2, EHHADH, PLD4, SRD5A2
GO:0006776~vitamin A metabolic process	5	0,006390061	RDH9, RDH11, DHRS9, RDH16, RETSAT
GO:0009719~response to endogenous stimulus	13	0,007726939	ME1, CAV1, IRS2, GCLC, INPPL1, LEPR, MMP14, SERPINA3N, SLC1A2, SPRR2D, HMOX1, SRD5A2, STEAP2
GO:0046942~carboxylic acid transport	9	0,008268153	SLC23A1, SLC1A2, PLIN2, SLC6A8, SLC25A22, PPARG, SLC22A5, SLC43A1, SLCO2A1
GO:0016101~diterpenoid metabolic process	5	0,008360908	RDH9, RDH11, DHRS9, RDH16, RETSAT
GO:0001523~retinoid metabolic process	5	0,008360908	RDH9, RDH11, DHRS9, RDH16, RETSAT
GO:0015849~organic acid transport	9	0,008765846	SLC23A1, SLC1A2, PLIN2, SLC6A8, SLC25A22, PPARG, SLC22A5, SLC43A1, SLCO2A1
GO:0009725~response to hormone stimulus	12	0,009008529	ME1, IRS2, SERPINA3N, CAV1, GCLC, SPRR2D, INPPL1, LEPR, HMOX1, SRD5A2, STEAP2, MMP14
GO:0009636~response to toxin	5	0,009480046	BAK1, CYP17A1, MT2, EPHX1, MT1
GO:0006721~terpenoid metabolic process	5	0,009480046	RDH9, RDH11, DHRS9, RDH16, RETSAT
GO:0046700~heterocycle catabolic process	6	0,010535436	HMOX1, ATP2A1, IDO2, CDA, MOXD1, PRODH
GO:0016126~sterol biosynthetic process	5	0,010692226	INSIG2, FDPS, HMGCS1, PMVK, SIGMAR1
GO:0006955~immune response	24	0,01096043	CXCL1, H2-Q5, C4A, INPPL1, PRG4, ENPP2, GBP9, H2-Q1, TLR5, OAS2, CXCL11, FCGR1, PSMB9, C1RB, CXCL13, CCL27A, GBP10, BCL6, H2-T10, C2, SPON2, CFD, DEFB1, IGH-VJ558
GO:0034622~cellular macromolecular complex assembly	14	0,011218661	PSMG1, HIST1H2BN, GM5620, TUBB2A, IPO4, GM6579, TUBB5, TUBA4A, H2AFX, HIST3H2A, HIST2H3C1, AGRN, PTBP2, SCO2
GO:0042905~9-cis-retinoic acid metabolic process	3	0,011757465	RDH9, DHRS9, RDH16
GO:0035238~vitamin A biosynthetic process	3	0,011757465	RDH9, DHRS9, RDH16
GO:0042904~9-cis-retinoic acid biosynthetic process	3	0,011757465	RDH9, DHRS9, RDH16
GO:0043627~response to estrogen stimulus	5	0,01491313	CAV1, SPRR2D, LEPR, HMOX1, MMP14
GO:0042445~hormone metabolic process	8	0,015957372	RDH9, RDH11, CYP17A1, DHRS9, SRD5A2, DIO1, RDH16, RETSAT
GO:0042362~fat-soluble vitamin biosynthetic process	3	0,016145297	RDH9, DHRS9, RDH16
GO:0006882~cellular zinc ion homeostasis	3	0,016145297	MT2, MT1, SLC39A4
GO:0006631~fatty acid metabolic process	12	0,019076745	SCD1, HACL1, ACNAT2, EHHADH, ACOT1, CRAT, ACACB, ACOT3, CYP4A10, ELOVL5, CYP4A32, ELOVL3, CYP4A31, FASN
GO:0065003~macromolecular complex assembly	18	0,020719239	CAV1, GM5620, TUBB2A, HIST2H3C1, PDSS2, PSMG1, HIST1H2BN, C1QTNF1, IPO4, GM6579, TUBB5, TUBA4A, CDA, HIST3H2A, H2AFX, AGRN, PTBP2, SCO2
GO:0055069~zinc ion homeostasis	3	0,021115923	MT2, MT1, SLC39A4
GO:0043933~macromolecular complex subunit organization	19	0,02219179	CAV1, GM5620, TUBB2A, HIST2H3C1, PDSS2, PSMG1, HIST1H2BN, C1QTNF1, IPO4, GM6579, APOA5, TUBB5, TUBA4A, CDA, HIST3H2A, H2AFX, AGRN, PTBP2, SCO2
GO:0006952~defense response	22	0,022599395	CXCL1, PNLIPRP2, C4A, PPARG, H2-Q1, SAA3, SAA4, TLR5, CXCL11, FCGR1, SERPINA3N, C1RB, SAA2, SAA1, CXCL13, IFNA14, C2, CFD, CLEC2H, DEFB1, ORM2, ORM3
GO:0048511~rhythmic process	8	0,024305948	SRRD, DBP, LEPR, PER2, PER3, ARNTL, NFIL3, MMP14
GO:0034621~cellular macromolecular complex subunit organization	14	0,027592702	PSMG1, HIST1H2BN, GM5620, TUBB2A, IPO4, GM6579, TUBB5, TUBA4A, H2AFX, HIST3H2A, HIST2H3C1, AGRN, PTBP2, SCO2
GO:0006695~cholesterol biosynthetic process	4	0,02823505	INSIG2, FDPS, HMGCS1, PMVK
GO:0006576~biogenic amine metabolic process	7	0,029095471	CHKA, OAZ1, IDO2, SLC22A5, FABP5, MOXD1, AMD2
GO:0032318~regulation of Ras GTPase activity	7	0,029095471	SPRY2, TBC1D17, AGFG2, ASAP2, BCL6, TBC1D30, ARAP2
GO:0048545~response to steroid hormone stimulus	6	0,030238489	CAV1, SPRR2D, LEPR, HMOX1, SRD5A2, MMP14
GO:0016054~organic acid catabolic process	7	0,030682228	HACL1, CYP39A1, CSAD, EHHADH, IDO2, MOXD1, PRODH
GO:0046395~carboxylic acid catabolic process	7	0,030682228	HACL1, CYP39A1, CSAD, EHHADH, IDO2, MOXD1, PRODH
GO:0043623~cellular protein complex assembly	8	0,038427693	PSMG1, GM5620, TUBB2A, IPO4, TUBB5, TUBA4A, AGRN, SCO2
GO:0009108~coenzyme biosynthetic process	6	0,038466651	DBT, GCLC, PDK4, ACSS2, PDSS2, COQ6
GO:0010033~response to organic substance	23	0,039630302	EGR1, VMN1R43, ME1, IRS2, CAV1, GCLC, INPPL1, VMN1R78, LEPR, PPARG, EPHX1, MMP14, ASAH1, VMN1R213, CCND1, SLC1A2, SERPINA3N, SPRR2D, HMOX1, VMN1R229, SRD5A2, ID3, STEAP2
GO:0051605~protein maturation by peptide bond cleavage	6	0,040717022	C1RB, C4A, SPCS2, C2, CFD, MMP14
GO:0031668~cellular response to extracellular stimulus	5	0,041437498	SREBF1, SLC1A2, LEPR, HMOX1, AVPR1A
GO:0030005~cellular di-, tri-valent inorganic cation homeostasis	9	0,042346274	BAK1, CAV1, PIK3CB, AVPR1A, MT2, MT1, GM5634, SLC39A4, SCO2
GO:0016485~protein processing	7	0,047524954	C1RB, C4A, APH1A, SPCS2, C2, CFD, MMP14
GO:0019748~secondary metabolic process	6	0,050503693	RDH9, RDH11, DHRS9, RDH16, HIBADH, RETSAT
GO:0015908~fatty acid transport	3	0,053455271	PLIN2, PPARG, SLCO2A1
GO:0042375~quinone cofactor metabolic process	3	0,053455271	CBR1, PDSS2, COQ6
GO:0043087~regulation of GTPase activity	7	0,054195842	SPRY2, TBC1D17, AGFG2, ASAP2, BCL6, TBC1D30, ARAP2
GO:0006603~phosphocreatine metabolic process	2	0,05743947	CKM, CKMT2
GO:0032764~negative regulation of mast cell cytokine production	2	0,05743947	HMOX1, BCL6
GO:0007263~nitric oxide mediated signal transduction	2	0,05743947	MT2, MT1
GO:0051336~regulation of hydrolase activity	11	0,060804258	SPRY2, BAK1, CAV1, TBC1D17, AGFG2, LEPR, ASAP2, NR4A1, BCL6, TBC1D30, ARAP2
GO:0001952~regulation of cell-matrix adhesion	3	0,061191367	PIK3CB, BCL6, MMP14
GO:0051604~protein maturation	7	0,061406499	C1RB, C4A, APH1A, SPCS2, C2, CFD, MMP14
GO:0055066~di-, tri-valent inorganic cation homeostasis	9	0,063855715	BAK1, CAV1, PIK3CB, AVPR1A, MT2, MT1, GM5634, SLC39A4, SCO2
GO:0070271~protein complex biogenesis	12	0,068810862	PSMG1, CAV1, GM5620, TUBB2A, C1QTNF1, IPO4, TUBB5, TUBA4A, CDA, AGRN, PDSS2, SCO2
GO:0006461~protein complex assembly	12	0,068810862	PSMG1, CAV1, GM5620, TUBB2A, C1QTNF1, IPO4, TUBB5, TUBA4A, CDA, AGRN, PDSS2, SCO2
GO:0006959~humoral immune response	5	0,071994449	C1RB, C4A, C2, CFD, IGH-VJ558
GO:0043086~negative regulation of catalytic activity	7	0,074628222	SPRY2, CDKN1A, CAV1, LEPR, NR4A1, GADD45B, ADORA1
GO:0030003~cellular cation homeostasis	9	0,076768476	BAK1, CAV1, PIK3CB, AVPR1A, MT2, MT1, GM5634, SLC39A4, SCO2
GO:0010817~regulation of hormone levels	8	0,080527382	RDH9, RDH11, CYP17A1, DHRS9, SRD5A2, DIO1, RDH16, RETSAT
GO:0002455~humoral immune response mediated by circulating immunoglobulin	4	0,081026302	C1RB, C4A, C2, IGH-VJ558
GO:0046578~regulation of Ras protein signal transduction	10	0,083073165	NGEF, SPRY2, TBC1D17, AGFG2, ARHGEF19, ASAP2, BCL6, TBC1D30, TTN, ARAP2
GO:0032763~regulation of mast cell cytokine production	2	0,084912897	HMOX1, BCL6
GO:0002719~negative regulation of cytokine production during immune response	2	0,084912897	HMOX1, BCL6
GO:0002701~negative regulation of production of molecular mediator of immune response	2	0,084912897	HMOX1, BCL6
GO:0010273~detoxification of copper ion	2	0,084912897	MT2, MT1
GO:0006820~anion transport	8	0,085797545	SLCO1A4, SLC16A1, SLC1A2, CLIC3, SLC17A1, CLIC5, SLC22A7, SLC25A22
GO:0042573~retinoic acid metabolic process	3	0,086412326	RDH9, DHRS9, RDH16
GO:0006956~complement activation	4	0,086568909	C1RB, C4A, C2, CFD
GO:0002541~activation of plasma proteins involved in acute inflammatory response	4	0,086568909	C1RB, C4A, C2, CFD
GO:0010927~cellular component assembly involved in morphogenesis	4	0,086568909	CD9, NEB, ACTA1, TTN

GO:0044092~negative regulation of molecular function	8	0,091260038	SPRY2, CDKN1A, CAV1, LEPR, HMOX1, NR4A1, GADD45B, ADORA1
GO:0007623~circadian rhythm	4	0,092267364	DBP, PER2, PER3, ARNTL
GO:0045087~innate immune response	7	0,092465628	C1RB, C4A, C2, TLR5, CFD, DEFB1, FCGR1
GO:0006936~muscle contraction	5	0,09726163	MYH2, MYH4, ACTN3, TTN, MAP2K6
GO:0002250~adaptive immune response	6	0,098370791	C1RB, C4A, BCL6, C2, FCGR1, IGH-VJ558
GO:0002460~adaptive immune response based on somatic recombination of immune receptors built	6	0,098370791	C1RB, C4A, BCL6, C2, FCGR1, IGH-VJ558

LKO-HFD

Term	Count	PValue	Genes
GO:0055114~oxidation reduction	60	1,33E-10	STEAP4, HTATIP2, ENOX2, CYP2J9, UTY, CYP2C69, PYROXD1, EHHADH, PGD, AKR1C12, AKR1C14, ERO1LB, CYP39A1, CYP7A1, HMOX1, SRD5A2, AKR7A5, GM9034, RTN4IP1, KDM5D, CYP3A44, CYP2C55, CYP2C54, CYP3A16, CYP3A11, CYP2B13, DHRS9, CBR4, MOXD1, COQ6, CYP4A32, ALDH1B1, CYP4A31, DLD, STEAP2, AKR1D1, RFESD, CYP2A4, ME1, HSD3B3, ACADSB, FDX1, ADH7, CBR1, CYP4A12A, FMO3, FASN, SCD1, CHDH, GPD1, CYP2D40, CYP4B1, CYP4A10, CYP7B1, DBT, CYP2A22, AOX1, DIO1, CYP4A14, RDH16, CYP2C38, RETSAT
GO:0016125~sterol metabolic process	14	3,10E-06	SREBF1, SOAT2, CYP7B1, CYP39A1, INSIG2, SAA1, LEPR, CYP7A1, PCTP, PCSK9, ABCA2, PMVK, SIGMAR1, SREBF2
GO:0008202~steroid metabolic process	20	5,00E-06	SREBF1, SOAT2, HSD3B3, STS, LEPR, PCTP, ABCA2, PMVK, SIGMAR1, SREBF2, CYP7B1, CYP39A1, INSIG2, SERPINA6, SULT1B1, SAA1, CYP7A1, PCSK9, SRD5A2, AKR1D1
GO:0008203~cholesterol metabolic process	13	6,29E-06	SREBF1, SOAT2, CYP7B1, CYP39A1, INSIG2, SAA1, LEPR, CYP7A1, PCTP, PCSK9, ABCA2, PMVK, SREBF2
GO:0016042~lipid catabolic process	16	9,06E-05	PNLIP, PNLIPRP1, PNLIPRP2, ENPP2, EHHADH, PLD4, PLBD2, CEL, CLPS, PLCB3, PLCE1, CYP39A1, CYP7A1, ASPG, SRD5A2, AKR1D1
GO:0048511~rhythmic process	13	1,94E-04	PRF1, CCRN4L, ENOX2, LEPR, ARNTL, MMP14, NR1D1, PTGDS, DBP, PER2, PER3, NFIL3, MTNR1A
GO:0007586~digestion	7	2,57E-04	PNLIP, CYP7B1, CLPS, PNLIPRP2, CYP39A1, PRSS2, CTRB1
GO:0007623~circadian rhythm	8	2,94E-04	PRF1, PTGDS, NR1D1, DBP, PER2, PER3, ARNTL, MTNR1A
GO:0006631~fatty acid metabolic process	17	9,63E-04	SCD1, ACADSB, EHHADH, ACNAT2, RNPEPL1, ACOT1, CBR4, CRAT, ACACB, ACSM3, CYP4A10, CYP4A12A, PTGDS, ELOVL5, CYP4A32, ELOVL3, CYP4A31, FASN, FABP4
GO:0008610~lipid biosynthetic process	22	0,001460315	SCD1, HSD3B3, CHKA, RNPEPL1, DHRS9, PISD, CBR4, ACACB, PMVK, SIGMAR1, ACSM3, CYP7B1, CYP39A1, PTGDS, INSIG2, ELOVL5, ELOVL3, FASN, SRD5A2, RDH16, AKR1D1, FABP5
GO:0009725~response to hormone stimulus	15	0,002462791	ME1, IRS2, PTPN2, LEPR, ABCA2, MMP14, IRS1, SERPINA3N, SPRR2D, HMOX1, ARSA, FABP4, PCSK9, SRD5A2, STEAP2
GO:0031669~cellular response to nutrient levels	6	0,002875466	SREBF1, ATG5, LEPR, HMOX1, PCSK9, ATG16L1
GO:0006706~steroid catabolic process	4	0,003270094	CYP39A1, CYP7A1, SRD5A2, AKR1D1
GO:0006953~acute-phase response	6	0,00393139	SERPINA3N, SAA2, SAA1, SAA3, SAA4, ORM2
GO:0046364~monosaccharide biosynthetic process	6	0,004551853	PGM3, GPD1, GNPDA1, GNPNAT1, PGD, GPI1
GO:0048545~response to steroid hormone stimulus	8	0,005440945	SPRR2D, LEPR, HMOX1, ARSA, FABP4, ABCA2, SRD5A2, MMP14
GO:0051186~cofactor metabolic process	15	0,005927102	GSTA1, MOCS2, EHHADH, ACNAT2, PDK4, PGD, ACOT1, ACSS2, COQ6, DBT, GGT6, CBR1, AK157302, HMOX1, NAPRT1
GO:0006041~glucosamine metabolic process	4	0,006088628	PGM3, GNPDA1, GNPNAT1, NAGK
GO:0006044~N-acetylglucosamine metabolic process	4	0,006088628	PGM3, GNPDA1, GNPNAT1, NAGK
GO:0009719~response to endogenous stimulus	15	0,006513145	ME1, IRS2, PTPN2, LEPR, ABCA2, MMP14, IRS1, SERPINA3N, SPRR2D, HMOX1, ARSA, FABP4, PCSK9, SRD5A2, STEAP2
GO:0006633~fatty acid biosynthetic process	9	0,008373097	ACSM3, SCD1, PTGDS, ELOVL5, ELOVL3, RNPEPL1, FASN, CBR4, ACACB
GO:0046165~alcohol biosynthetic process	6	0,009798086	PGM3, GPD1, GNPDA1, GNPNAT1, PGD, GPI1
GO:0046394~carboxylic acid biosynthetic process	12	0,012568217	ACSM3, SCD1, CYP7B1, CYP39A1, PTGDS, ELOVL5, ELOVL3, RNPEPL1, FASN, CBR4, ACACB, AKR1D1
GO:0016053~organic acid biosynthetic process	12	0,012568217	ACSM3, SCD1, CYP7B1, CYP39A1, PTGDS, ELOVL5, ELOVL3, RNPEPL1, FASN, CBR4, ACACB, AKR1D1
GO:0006694~steroid biosynthetic process	8	0,013406854	HSD3B3, CYP7B1, CYP39A1, INSIG2, SRD5A2, PMVK, SIGMAR1, AKR1D1
GO:0006732~coenzyme metabolic process	12	0,013855932	GSTA1, DBT, GGT6, MOCS2, ACNAT2, EHHADH, PGD, PDK4, ACOT1, ACSS2, NAPRT1, COQ6
GO:0043623~cellular protein complex assembly	10	0,015450479	PSMG2, GM5620, TUBB2A, TUBB5, TUBA4A, AGRN, SCO2, TUBA1C, MIS12, DVL1
GO:0044092~negative regulation of molecular function	11	0,02032446	CDKN1A, GTPBP4, LEPR, HMOX1, MLLT1, NR4A1, PCSK9, FABP4, HSPA1A, GADD45B, GADD45A
GO:0001525~angiogenesis	11	0,021301612	COL18A1, VEGFB, HTATIP2, TNFRSF12A, LEPR, HMOX1, RBPJ, MMP14, TNFAIP2, GPI1, CYR61
GO:0031668~cellular response to extracellular stimulus	6	0,021770525	SREBF1, ATG5, LEPR, HMOX1, PCSK9, ATG16L1
GO:0006914~autophagy	5	0,02383635	ATG5, ATG4A, ARSA, ATG16L1, ATG3
GO:0006882~cellular zinc ion homeostasis	3	0,023884716	MT2, MT1, SLC39A4
GO:0006699~bile acid biosynthetic process	3	0,023884716	CYP7B1, CYP39A1, AKR1D1
GO:0034622~cellular macromolecular complex assembly	15	0,024636243	HIST1H4M, GM5620, HIST1H2AF, TUBB2A, HIST2H3C1, H2AFJ, MIS12, DVL1, PSMG2, TUBB5, TUBA4A, AGRN, SMARCA2, SCO2, TUBA1C
GO:0002526~acute inflammatory response	8	0,025916314	SERPINA3N, C4A, SAA2, SAA1, SAA3, SAA4, CFD, ORM2
GO:0048514~blood vessel morphogenesis	14	0,02619392	COL18A1, HTATIP2, TNFRSF12A, LEPR, MMP14, GPI1, EPHA2, VEGFB, BAK1, ATG5, HMOX1, RBPJ, TNFAIP2, CYR61
GO:0009108~coenzyme biosynthetic process	7	0,026714765	DBT, GGT6, MOCS2, PDK4, ACSS2, NAPRT1, COQ6
GO:0043086~negative regulation of catalytic activity	9	0,028490371	CDKN1A, LEPR, MLLT1, NR4A1, PCSK9, FABP4, HSPA1A, GADD45B, GADD45A
GO:0006040~amino sugar metabolic process	4	0,028924894	PGM3, GNPDA1, GNPNAT1, NAGK
GO:0043627~response to estrogen stimulus	5	0,029320291	SPRR2D, LEPR, HMOX1, ARSA, MMP14
GO:0006575~cellular amino acid derivative metabolic process	11	0,030383462	GSTA1, CHKA, CHDH, GGT6, CKM, OAZ1, CSAD, AZIN1, SLC22A5, FABP5, MOXD1
GO:0034621~cellular macromolecular complex subunit organization	16	0,030847571	HIST1H4M, GM5620, HIST1H2AF, TUBB2A, HIST2H3C1, H2AFJ, MIS12, DVL1, PSMG2, MTRF1, TUBB5, TUBA4A, AGRN, SMARCA2, SCO2, TUBA1C
GO:0055069~zinc ion homeostasis	3	0,031099834	MT2, MT1, SLC39A4
GO:0006775~fat-soluble vitamin metabolic process	5	0,032319357	CBR1, DHRS9, ADH7, RDH16, RETSAT
GO:0006637~acyl-CoA metabolic process	4	0,03314704	DBT, ACNAT2, EHHADH, ACOT1
GO:0006766~vitamin metabolic process	7	0,036861161	CBR1, DHRS9, ADH7, SLC22A5, RDH16, NAPRT1, RETSAT
GO:0000075~cell cycle checkpoint	6	0,037856627	CCND1, BRCC3, PSMG2, FAM175A, TRRAP, ATR
GO:0034754~cellular hormone metabolic process	6	0,037856627	SERPINA6, DHRS9, ADH7, SRD5A2, RDH16, RETSAT
GO:0006412~translation	19	0,039116771	GM4342, RPSA, GM3362, GM5614, GM13680, RPL39, GM5908, GM5451, GM5093, GM7589, EIF4E, GM7429, MTRF1, RPS12, RPL3, RPL10, RPL5, RPL12, TARSL2, GM10154
GO:0010817~regulation of hormone levels	10	0,040626241	SERPINA6, LTBP4, DHRS9, ADH7, ILDR2, SRD5A2, DIO1, RDH16, IRS1, RETSAT
GO:0051726~regulation of cell cycle	14	0,044670959	GTPBP4, BRCC3, FAM175A, SIPA1, ATR, TRRAP, ATF5, BAK1, CCND1, CDKN1A, NUP214, PSMG2, GADD45B, GADD45A
GO:0051188~cofactor biosynthetic process	8	0,044700216	DBT, GGT6, MOCS2, AK157302, PDK4, ACSS2, NAPRT1, COQ6
GO:0009267~cellular response to starvation	4	0,04760741	SREBF1, ATG5, PCSK9, ATG16L1
GO:0034637~cellular carbohydrate biosynthetic process	6	0,049622279	PGM3, GPD1, GNPDA1, GNPNAT1, PGD, GPI1
GO:0051258~protein polymerization	5	0,053959277	GM5620, TUBB2A, TUBB5, TUBA4A, TUBA1C
GO:0009615~response to virus	7	0,054753535	LCN2, IFIH1, IFNA1, ISG15, POLR3K, IFNA5, H2-Q1, H2-Q9
GO:0051052~regulation of DNA metabolic process	6	0,056225668	GTPBP4, BRCC3, FAM175A, WRNIP1, BCL6, ID3
GO:0007162~negative regulation of cell adhesion	4	0,058692087	GTPBP4, BCL6, MMP14, CML5
GO:0006776~vitamin A metabolic process	4	0,064648555	DHRS9, ADH7, RDH16, RETSAT
GO:0006576~biogenic amine metabolic process	7	0,066976563	CHKA, CHDH, OAZ1, AZIN1, SLC22A5, FABP5, MOXD1
GO:0016052~carbohydrate catabolic process	7	0,07026138	GPD1, LYVE1, GNPDA1, PGD, CTBS, GM9034, GPI1
GO:0007263~nitric oxide mediated signal transduction	2	0,070398901	MT2, MT1
GO:0032764~negative regulation of mast cell cytokine production	2	0,070398901	HMOX1, BCL6
GO:0006045~N-acetylglucosamine biosynthetic process	2	0,070398901	PGM3, GNPNAT1
GO:0006042~glucosamine biosynthetic process	2	0,070398901	PGM3, GNPNAT1
GO:0006048~UDP-N-acetylglucosamine biosynthetic process	2	0,070398901	PGM3, GNPNAT1
GO:0030573~bile acid catabolic process	2	0,070398901	CYP39A1, AKR1D1
GO:0046854~phosphoinositide phosphorylation	3	0,077033713	PIK3C2G, PIK3CB, IP6K1
GO:0016051~carbohydrate biosynthetic process	7	0,07710508	PGM3, GPD1, GNPDA1, B3GALT1, GNPNAT1, PGD, GPI1
GO:0001523~retinoid metabolic process	4	0,077351611	DHRS9, ADH7, RDH16, RETSAT
GO:0016101~diterpenoid metabolic process	4	0,077351611	DHRS9, ADH7, RDH16, RETSAT
GO:0046164~alcohol catabolic process	6	0,08310718	GPD1, GNPDA1, PGD, ADH7, GM9034, GPI1
GO:0006721~terpenoid metabolic process	4	0,084081511	DHRS9, ADH7, RDH16, RETSAT
GO:0042594~response to starvation	4	0,084081511	SREBF1, ATG5, PCSK9, ATG16L1
GO:0043549~regulation of kinase activity	12	0,08499266	DGKA, CDKN1A, PLCE1, GTPBP4, MLLT1, FABP4, DGKH, KIT, GADD45B, GADD45A, IRS1, MAP2K6
GO:0001952~regulation of cell-matrix adhesion	3	0,087805937	PIK3CB, BCL6, MMP14
GO:0046834~lipid phosphorylation	3	0,087805937	PIK3C2G, PIK3CB, IP6K1
GO:0000077~DNA damage checkpoint	4	0,091051898	CCND1, BRCC3, FAM175A, ATR
GO:0046486~glycerolipid metabolic process	9	0,092272221	CHKA, PIK3C2G, INSIG2, PIK3CB, PCSK9, PIP5K1C, DGKH, IP6K1, FABP5
GO:0010212~response to ionizing radiation	5	0,092320876	BAK1, BRCC3, FAM175A, NEK1, XRCC6
GO:0008206~bile acid metabolic process	3	0,098992293	CYP7B1, CYP39A1, AKR1D1

LKO-CT and LKO-HFD

Term	Count	PValue	Genes
GO:0055114~oxidation reduction	23	3,12E-09	STEAP4, CYP2C55, CYP3A16, HTATIP2, CYP2D40, CYP2J9, CYP3A11, EHHADH, DHRS9, CYP2B13, MOXD1, CYP4A10, CYP2A22, CYP7B1, CBR1, HMOX1, FMO3, AOX1, CYP4A31, CYP2C38, RDH16, CYP4A14, CYP3A44, CYP2A4
GO:0007586~digestion	5	3,79E-05	PNLIP, CYP7B1, CLPS, PNLIPRP2, CTRB1
GO:0006953~acute-phase response	5	6,79E-05	SERPINA3N, SAA2, SAA1, SAA3, ORM2
GO:0002526~acute inflammatory response	6	3,36E-04	SERPINA3N, C4A, SAA2, SAA1, SAA3, ORM2
GO:0016042~lipid catabolic process	7	4,84E-04	PNLIP, CEL, CLPS, PNLIPRP1, PNLIPRP2, EHHADH, PLBD2
GO:0006954~inflammatory response	8	0,001431859	CXCL1, SERPINA3N, C4A, SAA2, SAA1, SAA3, CXCL11, ORM2
GO:0051186~cofactor metabolic process	7	0,002354936	GSTA1, CBR1, AK157302, HMOX1, EHHADH, PDK4, ACOT1
GO:0006575~cellular amino acid derivative metabolic process	6	0,00400093	GSTA1, CHKA, OAZ1, CSAD, SLC22A5, MOXD1
GO:0006952~defense response	10	0,006090473	CXCL1, SERPINA3N, PNLIPRP2, C4A, SAA2, SAA1, H2-Q1, SAA3, CXCL11, ORM2
GO:0006955~immune response	10	0,00834408	CXCL1, C4A, GP49A, PRG4, H2-Q1, GBP10, BCL6, H2-T10, SPON2, CXCL11
GO:0006766~vitamin metabolic process	4	0,014654283	CBR1, DHRS9, SLC22A5, RDH16
GO:0009611~response to wounding	8	0,014798346	CXCL1, SERPINA3N, C4A, SAA2, SAA1, SAA3, CXCL11, ORM2
GO:0032764~negative regulation of mast cell cytokine production	2	0,014811351	HMOX1, BCL6
GO:0007263~nitric oxide mediated signal transduction	2	0,014811351	MT2, MT1
GO:0006508~proteolysis	15	0,020505937	CELA3B, SOCS2, C4A, CTRB1, TRY4, KLK1, CELA1, XRCC6BP1, CPA2, 2210010C04RIK, GM5409, CELA2A, CPA1, CPB1, CTRL
GO:0006576~biogenic amine metabolic process	4	0,021678156	CHKA, OAZ1, SLC22A5, MOXD1
GO:0032763~regulation of mast cell cytokine production	2	0,022135365	HMOX1, BCL6
GO:0002719~negative regulation of cytokine production during immune response	2	0,022135365	HMOX1, BCL6
GO:0002701~negative regulation of production of molecular mediator of immune response	2	0,022135365	HMOX1, BCL6
GO:0010273~detoxification of copper ion	2	0,022135365	MT2, MT1
GO:0006775~fat-soluble vitamin metabolic process	3	0,02629779	CBR1, DHRS9, RDH16
GO:0042904~9-cis-retinoic acid biosynthetic process	2	0,043785501	DHRS9, RDH16
GO:0042905~9-cis-retinoic acid metabolic process	2	0,043785501	DHRS9, RDH16
GO:0035238~vitamin A biosynthetic process	2	0,043785501	DHRS9, RDH16
GO:0042362~fat-soluble vitamin biosynthetic process	2	0,050896211	DHRS9, RDH16
GO:0046688~response to copper ion	2	0,050896211	MT2, MT1
GO:0006882~cellular zinc ion homeostasis	2	0,050896211	MT2, MT1
GO:0002718~regulation of cytokine production during immune response	2	0,050896211	HMOX1, BCL6
GO:0055069~zinc ion homeostasis	2	0,057954563	MT2, MT1
GO:0006732~coenzyme metabolic process	4	0,090570537	GSTA1, EHHADH, PDK4, ACOT1
GO:0002703~regulation of leukocyte mediated immunity	3	0,095478048	HMOX1, H2-Q1, BCL6

LKO-CT and WT-HFD

Term	Count	PValue	Genes
GO:0055114~oxidation reduction	23	2,35E-10	STEAP4, CYP2C55, CYP3A16, HTATIP2, CYP2D40, CYP2J9, CYP3A11, EHHADH, DHRS9, CYP2B13, MOXD1, CYP4A10, CYP2A22, CYP7B1, CBR1, HMOX1, FMO3, AOX1, CYP4A31, CYP2C38, RDH16, CYP4A14, CYP3A44, CYP2A4
GO:0007586~digestion	5	2,30E-05	PNLIP, CYP7B1, CLPS, PNLIPRP2, CTRB1
GO:0006953~acute-phase response	5	4,14E-05	SERPINA3N, SAA2, SAA1, SAA3, ORM2
GO:0002526~acute inflammatory response	6	1,86E-04	SERPINA3N, C4A, SAA2, SAA1, SAA3, ORM2
GO:0006575~cellular amino acid derivative metabolic process	7	3,22E-04	GSTA1, CHKA, OAZ1, CSAD, SLC22A5, FABP5, MOXD1
GO:0006954~inflammatory response	8	6,78E-04	CXCL1, SERPINA3N, C4A, SAA2, SAA1, SAA3, CXCL11, ORM2
GO:0016042~lipid catabolic process	6	0,00185219	PNLIP, CEL, CLPS, PNLIPRP1, PNLIPRP2, EHHADH
GO:0006576~biogenic amine metabolic process	5	0,001861565	CHKA, OAZ1, SLC22A5, FABP5, MOXD1
GO:0006952~defense response	10	0,002617232	CXCL1, SERPINA3N, PNLIPRP2, C4A, SAA2, SAA1, H2-Q1, SAA3, CXCL11, ORM2
GO:0051186~cofactor metabolic process	6	0,006842051	GSTA1, CBR1, HMOX1, EHHADH, PDK4, ACOT1
GO:0009611~response to wounding	8	0,007667599	CXCL1, SERPINA3N, C4A, SAA2, SAA1, SAA3, CXCL11, ORM2
GO:0006766~vitamin metabolic process	4	0,010425105	CBR1, DHRS9, SLC22A5, RDH16
GO:0006955~immune response	9	0,011945061	CXCL1, C4A, PRG4, H2-Q1, GBP10, BCL6, H2-T10, SPON2, CXCL11
GO:0032764~negative regulation of mast cell cytokine production	2	0,013057372	HMOX1, BCL6
GO:0007263~nitric oxide mediated signal transduction	2	0,013057372	MT2, MT1
GO:0006508~proteolysis	14	0,016787105	CELA3B, SOCS2, C4A, CTRB1, TRY4, KLK1, CELA1, XRCC6BP1, CPA2, GM5409, CPA1, CELA2A, CPB1, CTRL
GO:0002719~negative regulation of cytokine production during immune response	2	0,019522696	HMOX1, BCL6
GO:0032763~regulation of mast cell cytokine production	2	0,019522696	HMOX1, BCL6
GO:0010273~detoxification of copper ion	2	0,019522696	MT2, MT1
GO:0002701~negative regulation of production of molecular mediator of immune response	2	0,019522696	HMOX1, BCL6
GO:0006775~fat-soluble vitamin metabolic process	3	0,020775402	CBR1, DHRS9, RDH16
GO:0035238~vitamin A biosynthetic process	2	0,038668456	DHRS9, RDH16
GO:0042905~9-cis-retinoic acid metabolic process	2	0,038668456	DHRS9, RDH16
GO:0042904~9-cis-retinoic acid biosynthetic process	2	0,038668456	DHRS9, RDH16
GO:0046688~response to copper ion	2	0,04496786	MT2, MT1
GO:0006882~cellular zinc ion homeostasis	2	0,04496786	MT2, MT1
GO:0042362~fat-soluble vitamin biosynthetic process	2	0,04496786	DHRS9, RDH16
GO:0002718~regulation of cytokine production during immune response	2	0,04496786	HMOX1, BCL6
GO:0006656~phosphatidylcholine biosynthetic process	2	0,04496786	CHKA, FABP5
GO:0055069~zinc ion homeostasis	2	0,051226446	MT2, MT1
GO:0006732~coenzyme metabolic process	4	0,06744846	GSTA1, EHHADH, PDK4, ACOT1
GO:0046470~phosphatidylcholine metabolic process	2	0,075857818	CHKA, FABP5
GO:0002703~regulation of leukocyte mediated immunity	3	0,076959002	HMOX1, H2-Q1, BCL6
GO:0016054~organic acid catabolic process	3	0,098673184	CSAD, EHHADH, MOXD1
GO:0046395~carboxylic acid catabolic process	3	0,098673184	CSAD, EHHADH, MOXD1

WT-HFD and LKO-HFD

Term	Count	PValue	Genes
GO:0055114~oxidation reduction	38	2,40E-11	ME1, STEAP4, HSD3B3, HTATIP2, CYP2J9, EHHADH, CBR1, CYP39A1, CYP3A41B, HMOX1, FMO3, CYP3A41A, FASN, SRD5A2, CYP3A44, SCD1, CYP2C55, CYP2C54, CYP3A16, CYP2D40, CYP3A11, DHRS9, CYP2B13, MOXD1, CYP4B1, COQ6, CYP4A10, CYP7B1, CYP2A22, DBT, CYP4A32, ALDH1B1, AOX1, CYP4A31, DIO1, RDH16, STEAP2, CYP4A14, CYP2C38, CYP2A4, RETSAT
GO:0016125~sterol metabolic process	9	2,84E-05	SREBF1, SOAT2, CYP7B1, CYP39A1, INSIG2, SAA1, LEPR, PMVK, SIGMAR1
GO:0007586~digestion	6	4,75E-05	PNLIP, CYP7B1, CLPS, PNLIPRP2, CYP39A1, CTRB1
GO:0008610~lipid biosynthetic process	16	4,86E-05	SCD1, HSD3B3, CHKA, DHRS9, ACACB, PMVK, SIGMAR1, CYP7B1, CYP39A1, ELOVL5, INSIG2, ELOVL3, FASN, SRD5A2, RDH16, FABP5
GO:0008202~steroid metabolic process	12	5,04E-05	SREBF1, SOAT2, HSD3B3, CYP7B1, CYP39A1, INSIG2, SULT1B1, SAA1, LEPR, SRD5A2, PMVK, SIGMAR1
GO:0006953~acute-phase response	6	9,77E-05	SERPINA3N, SAA2, SAA1, SAA3, SAA4, ORM2
GO:0008203~cholesterol metabolic process	8	1,16E-04	SREBF1, SOAT2, CYP7B1, CYP39A1, INSIG2, SAA1, LEPR, PMVK
GO:0016042~lipid catabolic process	10	2,78E-04	PNLIP, CEL, CLPS, PNLIPRP1, PNLIPRP2, CYP39A1, ENPP2, EHHADH, PLD4, SRD5A2
GO:0002526~acute inflammatory response	8	2,90E-04	SERPINA3N, C4A, SAA2, SAA1, SAA3, SAA4, CFD, ORM2
GO:0006694~steroid biosynthetic process	7	8,90E-04	HSD3B3, CYP7B1, CYP39A1, INSIG2, SRD5A2, PMVK, SIGMAR1
GO:0051186~cofactor metabolic process	10	0,00244137	GSTA1, DBT, CBR1, ACNAT2, HMOX1, EHHADH, PDK4, ACOT1, ACSS2, COQ6
GO:0006631~fatty acid metabolic process	10	0,002626859	CYP4A10, SCD1, CYP4A32, ELOVL5, ACNAT2, ELOVL3, EHHADH, CYP4A31, FASN, ACOT1, ACACB, CRAT
GO:0006954~inflammatory response	11	0,003128643	CXCL1, SERPINA3N, C4A, SAA2, CXCL13, SAA1, SAA3, SAA4, CFD, CXCL11, ORM2
GO:0009611~response to wounding	14	0,003566188	CXCL1, F11, SERPINA3N, C4A, SAA2, PIK3CB, SAA1, CXCL13, SAA3, SAA4, ID3, CFD, CXCL11, ORM2
GO:0006637~acyl-CoA metabolic process	4	0,003650599	DBT, ACNAT2, EHHADH, ACOT1
GO:0048511~rhythmic process	7	0,004604549	DBP, LEPR, PER2, PER3, ARNTL, NFIL3, MMP14
GO:0009725~response to hormone stimulus	9	0,004723435	ME1, IRS2, SERPINA3N, SPRR2D, LEPR, HMOX1, SRD5A2, STEAP2, MMP14
GO:0006882~cellular zinc ion homeostasis	3	0,004966324	MT2, MT1, SLC39A4
GO:0055069~zinc ion homeostasis	3	0,006552995	MT2, MT1, SLC39A4
GO:0006732~coenzyme metabolic process	8	0,007686465	GSTA1, DBT, ACNAT2, EHHADH, PDK4, ACOT1, ACSS2, COQ6
GO:0006955~immune response	16	0,008017833	CXCL1, H2-Q5, C4A, PRG4, ENPP2, H2-Q1, GBP9, CXCL11, PSMB9, CXCL13, GBP10, BCL6, H2-T10, CFD, SPON2, DEFB1
GO:0009719~response to endogenous stimulus	9	0,00892319	ME1, IRS2, SERPINA3N, SPRR2D, LEPR, HMOX1, SRD5A2, STEAP2, MMP14
GO:0006952~defense response	15	0,01214761	CXCL1, SERPINA3N, PNLIPRP2, C4A, SAA2, SAA1, CXCL13, H2-Q1, SAA3, SAA4, CLEC2H, CFD, CXCL11, DEFB1, ORM2
GO:0048545~response to steroid hormone stimulus	5	0,014902633	SPRR2D, LEPR, HMOX1, SRD5A2, MMP14
GO:0043627~response to estrogen stimulus	4	0,015032404	SPRR2D, LEPR, HMOX1, MMP14
GO:0006775~fat-soluble vitamin metabolic process	4	0,01629861	CBR1, DHRS9, RDH16, RETSAT
GO:0001952~regulation of cell-matrix adhesion	3	0,020009831	PIK3CB, BCL6, MMP14
GO:0046942~carboxylic acid transport	6	0,020417819	SLC23A1, SLC6A8, SLC25A22, SLC22A5, SLC43A1, SLCO2A1
GO:0007623~circadian rhythm	4	0,020446521	DBP, PER2, PER3, ARNTL
GO:0015849~organic acid transport	6	0,02122502	SLC23A1, SLC6A8, SLC25A22, SLC22A5, SLC43A1, SLCO2A1
GO:0006766~vitamin metabolic process	5	0,023690088	CBR1, DHRS9, SLC22A5, RDH16, RETSAT
GO:0046394~carboxylic acid biosynthetic process	7	0,024634335	SCD1, CYP7B1, CYP39A1, ELOVL5, ELOVL3, FASN, ACACB
GO:0006575~cellular amino acid derivative metabolic process	7	0,024634335	GSTA1, CHKA, OAZ1, CSAD, SLC22A5, FABP5, MOXD1
GO:0016053~organic acid biosynthetic process	7	0,024634335	SCD1, CYP7B1, CYP39A1, ELOVL5, ELOVL3, FASN, ACACB
GO:0051258~protein polymerization	4	0,025120721	GM5620, TUBB2A, TUBB5, TUBA4A
GO:0043623~cellular protein complex assembly	6	0,02843582	GM5620, TUBB2A, TUBB5, TUBA4A, AGRN, SCO2
GO:0032764~negative regulation of mast cell cytokine production	2	0,031396355	HMOX1, BCL6
GO:0007263~nitric oxide mediated signal transduction	2	0,031396355	MT2, MT1
GO:0006576~biogenic amine metabolic process	5	0,037961369	CHKA, OAZ1, SLC22A5, FABP5, MOXD1
GO:0006633~fatty acid biosynthetic process	5	0,039456938	SCD1, ELOVL5, ELOVL3, FASN, ACACB
GO:0002719~negative regulation of cytokine production during immune response	2	0,046724618	HMOX1, BCL6
GO:0032763~regulation of mast cell cytokine production	2	0,046724618	HMOX1, BCL6
GO:0002701~negative regulation of production of molecular mediator of immune response	2	0,046724618	HMOX1, BCL6
GO:0010273~detoxification of copper ion	2	0,046724618	MT2, MT1
GO:0034754~cellular hormone metabolic process	4	0,049017847	DHRS9, SRD5A2, RDH16, RETSAT
GO:0042445~hormone metabolic process	5	0,05441168	DHRS9, SRD5A2, DIO1, RDH16, RETSAT
GO:0030005~cellular di-, tri-valent inorganic cation homeostasis	6	0,061700166	BAK1, PIK3CB, MT2, MT1, SLC39A4, SCO2
GO:0006776~vitamin A metabolic process	3	0,063178891	DHRS9, RDH16, RETSAT
GO:0031669~cellular response to nutrient levels	3	0,07200233	SREBF1, LEPR, HMOX1
GO:0016101~diterpenoid metabolic process	3	0,07200233	DHRS9, RDH16, RETSAT
GO:0001523~retinoid metabolic process	3	0,07200233	DHRS9, RDH16, RETSAT
GO:0009636~response to toxin	3	0,07655491	BAK1, MT2, MT1
GO:0006721~terpenoid metabolic process	3	0,07655491	DHRS9, RDH16, RETSAT
GO:0009108~coenzyme biosynthetic process	4	0,080729556	DBT, PDK4, ACSS2, COQ6
GO:0016126~sterol biosynthetic process	3	0,08119601	INSIG2, PMVK, SIGMAR1
GO:0055066~di-, tri-valent inorganic cation homeostasis	6	0,082269212	BAK1, PIK3CB, MT2, MT1, SLC39A4, SCO2
GO:0051336~regulation of hydrolase activity	7	0,090547001	BAK1, AGFG2, LEPR, ASAP2, NR4A1, BCL6, TBC1D30
GO:0006085~acetyl-CoA biosynthetic process	2	0,091275727	PDK4, ACSS2
GO:0042904~9-cis-retinoic acid biosynthetic process	2	0,091275727	DHRS9, RDH16
GO:0001953~negative regulation of cell-matrix adhesion	2	0,091275727	BCL6, MMP14
GO:0035238~vitamin A biosynthetic process	2	0,091275727	DHRS9, RDH16
GO:0042905~9-cis-retinoic acid metabolic process	2	0,091275727	DHRS9, RDH16
GO:0030003~cellular cation homeostasis	6	0,093762989	BAK1, PIK3CB, MT2, MT1, SLC39A4, SCO2
GO:0006508~proteolysis	23	0,09503672	F11, CELA3B, C4A, SOCS2, USP2, CTRB1, MAN1B1, TRY4, KLK1, CELA1, MMP14, XRCC6BP1, PSMB9, CASP7, BACE1, CPA2, NEDD4L, GM5409, CELA2A, CPA1, CPB1, CFD, CTRL
GO:0000041~transition metal ion transport	4	0,09919073	STEAP4, STEAP2, SLC39A4, SCO2

LKO-CT, WT-HFD and LKO-HFD

Term	Count	PValue	Genes
GO:0055114~oxidation reduction	23	1,85E-10	STEAP4, CYP2C55, CYP3A16, HTATIP2, CYP2D40, CYP2J9, CYP3A11, EHHADH, DHRS9, CYP2B13, MOXD1, CYP4A10, CYP2A22, CYP7B1, CBR1, HMOX1, FMO3, AOX1, CYP4A31, CYP2C38, RDH16, CYP4A14, CYP3A44, CYP2A4
GO:0007586~digestion	5	2,20E-05	PNLIP, CYP7B1, CLPS, PNLIPRP2, CTRB1
GO:0006953~acute-phase response	5	3,96E-05	SERPINA3N, SAA2, SAA1, SAA3, ORM2
GO:0002526~acute inflammatory response	6	1,77E-04	SERPINA3N, C4A, SAA2, SAA1, SAA3, ORM2
GO:0006954~inflammatory response	8	6,33E-04	CXCL1, SERPINA3N, C4A, SAA2, SAA1, SAA3, CXCL11, ORM2
GO:0016042~lipid catabolic process	6	0,001761866	PNLIP, CEL, CLPS, PNLIPRP1, PNLIPRP2, EHHADH
GO:0006575~cellular amino acid derivative metabolic process	6	0,002202253	GSTA1, CHKA, OAZ1, CSAD, SLC22A5, MOXD1
GO:0006952~defense response	10	0,002421346	CXCL1, SERPINA3N, PNLIPRP2, C4A, SAA2, SAA1, H2-Q1, SAA3, CXCL11, ORM2
GO:0051186~cofactor metabolic process	6	0,006526868	GSTA1, CBR1, HMOX1, EHHADH, PDK4, ACOT1
GO:0009611~response to wounding	8	0,007218081	CXCL1, SERPINA3N, C4A, SAA2, SAA1, SAA3, CXCL11, ORM2
GO:0006766~vitamin metabolic process	4	0,01010992	CBR1, DHRS9, SLC22A5, RDH16
GO:0006955~immune response	9	0,01119936	CXCL1, C4A, PRG4, H2-Q1, GBP10, BCL6, H2-T10, SPON2, CXCL11
GO:0032764~negative regulation of mast cell cytokine production	2	0,012911136	HMOX1, BCL6
GO:0007263~nitric oxide mediated signal transduction	2	0,012911136	MT2, MT1
GO:0006576~biogenic amine metabolic process	4	0,015069119	CHKA, OAZ1, SLC22A5, MOXD1
GO:0006508~proteolysis	14	0,015369173	CELA3B, SOCS2, C4A, CTRB1, TRY4, KLK1, CELA1, XRCC6BP1, CPA2, CPA1, CELA2A, GM5409, CPB1, CTRL
GO:0032763~regulation of mast cell cytokine production	2	0,019304764	HMOX1, BCL6
GO:0002701~negative regulation of production of molecular mediator of immune response	2	0,019304764	HMOX1, BCL6
GO:0010273~detoxification of copper ion	2	0,019304764	MT2, MT1
GO:0002719~negative regulation of cytokine production during immune response	2	0,019304764	HMOX1, BCL6
GO:0006775~fat-soluble vitamin metabolic process	3	0,020340077	CBR1, DHRS9, RDH16
GO:0035238~vitamin A biosynthetic process	2	0,038241007	DHRS9, RDH16
GO:0042905~9-cis-retinoic acid metabolic process	2	0,038241007	DHRS9, RDH16
GO:0042904~9-cis-retinoic acid biosynthetic process	2	0,038241007	DHRS9, RDH16
GO:0042362~fat-soluble vitamin biosynthetic process	2	0,044472401	DHRS9, RDH16
GO:0046688~response to copper ion	2	0,044472401	MT2, MT1
GO:0002718~regulation of cytokine production during immune response	2	0,044472401	HMOX1, BCL6
GO:0006882~cellular zinc ion homeostasis	2	0,044472401	MT2, MT1
GO:0055069~zinc ion homeostasis	2	0,050663877	MT2, MT1
GO:0006732~coenzyme metabolic process	4	0,065660644	GSTA1, EHHADH, PDK4, ACOT1
GO:0002703~regulation of leukocyte mediated immunity	3	0,075473207	HMOX1, H2-Q1, BCL6
GO:0046395~carboxylic acid catabolic process	3	0,096816533	CSAD, EHHADH, MOXD1
GO:0016054~organic acid catabolic process	3	0,096816533	CSAD, EHHADH, MOXD1

Supplementary online Material and Methods.

Mice were anaesthetized with isoflurane (Forene®, Abbott, Queenborough, Kent, England) after a 5 h-fast. Portal and cava vein blood samples were harvested for further analysis. After exsanguination, the mice were killed by cervical dislocation, and tissues were sampled. Adipose tissue deposits (mesenteric, epididymal, and subcutaneous), the liver, intestinal segments and the *tibialis anterior* (TA) skeletal muscles were precisely dissected, weighed, immediately immersed in liquid nitrogen and stored at -80°C until further analysis.

Indirect calorimetry studies in metabolic chambers

A set of 10 weeks-old WT and LKO mice were fed a control diet (CT) (10% fat, AIN93Mi, Research Diet, New Brunswick, NJ, USA) (WT-CT or LKO-CT) or a high-fat diet (HFD) (60% fat, D12492i Research Diet, New Brunswick, NJ, USA) (WT-HFD or LKO-HFD) (20 mice, n=4-6/group) for 8 weeks. The mice were then placed for one week in metabolic chambers (Labmaster, TSE Systems GmbH, Bad Homburg, Germany). Mice were housed individually, with free access to food and water. VO_2, VCO_2, physical activity and total energy expenditure were precisely recorded for 5 consecutive days.

Microarray analysis

Equal amounts of RNA from at least 10 mice per group were pooled within each group. Microarrays were performed as previously described [1]. The expression profile of several genes (up to 25) has been confirmed by using qPCR from individual animals, not from a pool of RNA. Mouse gene ST microarray chips were used for hybridization (MoGene 2.0 ST, Affymetrix®) the total number of genes covered by the probes is about 35240 genes, 28960 passed the signal filter. A GeneChip WT PLUS Reagent Kit (Affymetrix ®) was used for cRNA preparation from total RNA. Hybridization, washing and scanning were performed

according to the Affymetrix kits and procedures specific to the mouse gene ST chips. After the scanning was complete, the hybridization quality controls were checked using Affymetrix Gene Expression Console software. Using the Affymetrix APT suite tools, we normalized the data by the RMA-Sketch procedure and computed the signal detection p-values using the DABG algorithm. All the probe sets that had a DABG p-value above 0.05 in all conditions were discarded from the analysis. The rest of the probe sets were kept for fold-change analysis. Functional annotation and pathway analysis were performed using the DAVID web tool [2]. The prediction of the transcription factors regulated (inhibited or activated) by the different conditions was made using the TFactS web tool [3]. Analyses using both web tools were performed with a list of selected official gene names (the selection of genes was made using the threshold of 1.5-fold change versus WT-CT or versus WT-HFD) as input, and the threshold of significance was set by default to p-values below 0.05. All the graphs (Venn diagram, heat map and bar plot) related to the microarray analysis were generated using R scripts.

DNA isolation from mouse caecal samples for sequencing

Caecal contents were collected and kept frozen at -80°C until use. Metagenomic DNA was extracted from the caecal content using a QIAamp DNA Stool Mini Kit (Qiagen, Hilden, Germany) according to the manufacturer's instructions with modifications [4].

Bacterial DNA sequencing

The 16S rRNA gene was amplified from the caecal microbiota of the mice using the following universal eubacterial primers: 27Fmod (5'-AGRGTTTGATCMTGGCTCAG-3') and 519Rmodbio (5'-GTNTTACNGCGGCKGCTG-3'). Purified amplicons were sequenced utilizing Roche 454 FLX titanium instruments and reagents following the manufacturer's guidelines. Sequencing was performed at MR DNA (www.mrdnalab.com, Shallowater, TX,

USA). The number of raw sequences from the sequencing output was 1070821. Sequences were demultiplexed and processed using the QIIME pipeline (v1.7 using default options (Q25, minimum sequence lenght = 200 bp, maximum sequence length = 1000 bp, maximum number of ambiguous bases = 6, maximum number of homopolymers = 6, maximum number of primer mismatchs = 0). After quality processing, 957250 sequences (83.4%) remained. For the 48 samples analyzed, 43881 OTUs have been identified (97% similarity). The minimum number of sequences per sample was 9741 and the maximum number of sequences per sample was 29605. The median number of sequences per sample was 20886 and the mean number of sequences per sample was 19942.71 +/- 5027.019 (standard deviation). The Q25 sequence data derived from the sequencing process were analyzed with the QIIME 1.7 pipeline.

Briefly, sequences were depleted of barcodes and primers. Sequences <200 bp or >1000 bp were then removed; sequences with ambiguous base calls and with homopolymer runs exceeding 6 bp were also removed. Sequences were denoised, and operational taxonomic units (OTUs) were generated. Chimeras were also removed. OTUs were defined by clustering at 3% divergence (97% similarity). Final OTUs were taxonomically classified using BLASTn against a curated Greengenes database. PCoA was generated with QIIME using the unweighted UniFrac distance matrix between the samples [5, 6] and as previously described [7, 8].

Oral glucose tolerance test (OGTT)

After the mice underwent 7 weeks of treatment, an OGTT was performed as previously described [7].

Insulin tolerance test (ITT)

After the mice underwent 7 weeks of treatment, 5 hour-fasted mice were intraperitoneally injected with insulin (0.75 mU/g). Blood was collected from the tail vein at time 0 and after 15, 30, 45, 60 min for determination of glucose levels.

Insulin resistance index

The insulin concentrations in plasma samples collected from tail blood during OGTT were measured using an ELISA kit (Mercodia, Uppsala, Sweden) according to the manufacturer's instructions. The insulin resistance index was calculated by multiplying the area under the curve of both the blood glucose (-30 to 120 min) and the plasma insulin (-30 to 15 min) obtained from the OGTT.

Insulin signaling

To analyze the insulin signaling pathway, mice received insulin 1mU/g (Actrapid; Novo Nordisk A/S, Denmark) under anesthesia (isoflurane, Forene®, Abbott, Queenborough, Kent, England), or an equal volume of PBS into the portal vein to analyze signaling response to insulin. Three min after injection, mice were euthanized and liver were rapidly dissected.

Plasma ALT/AST

Plasma alanine-aminostransferase (ALT) and aspartate-aminotransferase (AST) activities were measured using kits coupling the enzymatic activity of interest with a $NADH+H^+$-dependent enzymatic reaction and spectrophotometric detection of $NADH+H^+$ conversion to NAD^+ (Diasys Diagnostic Systems, Holzheim, Germany) according to the manufacturer's instructions.

Liver lipid content

Total lipids were measured in the liver tissue after extraction in $CHCl_3$:MeOH according to Folch et al. [9] and adapted as previously described [10]. Briefly, 100 mg of liver tissue was homogenized in 1 ml of phosphate buffer (pH 7.4) using Ultra-Turrax (IKA, T10 basic, Boutersem, Belgium) until complete tissue lysis. Lipids were extracted by mixing 125 µl of lysates with 1 ml of $CHCl_3$:MeOH (2:1). The chloroform phase was evaporated under nitrogen flux, and the dried residue was solubilized in 100 µl of isopropanol. Triglycerides were measured using kits coupling enzymatic reaction and spectrophotometric detection of reaction end products (Diasys Diagnostic and Systems, Holzheim, Germany). Protein concentrations were measured by the Bradford method using bovine serum albumin as a standard.

Histological analysis

Slides preparation

A fraction of the main liver lobe was mounted in OCT embedding medium (Tissue-tek, Sakura, The Netherlands), sliced in 5µm thick sections and stored at -80°C until further analysis. Before histological staining, the frozen tissue sections were fixed in ice-cold 4% formaldehyde solution diluted in methanol for 5min.

Stainings

Liver steatosis was visualized by Oil Red O staining. The sections were stained with 0.5% Oil red O solution in propylene glycol for 10 min at 60°C. The slides were transferred to an 85% propylene glycol solution for 1 min, rinsed in distilled water for 2 changes, and processed for hematoxylin counter staining. The sections were then cleared in Xylene, mounted with DPX and coverslipped.

Liver fibrosis was visualized by Picrosirius red. The samples were incubated for 90 min in 0.1% Sirius red F3B (Sigma) dissolved in saturated picric acid. After rinsing twice in acidified water and in distilled water, sections were briefly dehydrated with increasing concentrations of ethanol. The sections were then cleared in Xylene, mounted with DPX and coverslipped.

General morphology of the liver was assessed on Hematoxylin and Eosin (H&E) stained sections using a standard protocol.

To visualize inflammatory cells a F4/80 staining was performed. After fixation, endogenous peroxidase activity was quenched with 0.3 % H_2O_2 in methanol for 20 minutes. Following blocking in TSA TNB (Perkin Elmer, Waltham, MA, USA) for 1 hour, sections were incubated overnight with specific rat anti-mouse primary antibodies directed against F4/80 (1:100; ab6640, Abcam, Cambridge, England) at room temperature. The following day, slides were incubated with a rabbit anti-rat secondary antibody for 2h (1:200; 312-065-003, Jackson ImmunoResearch Laboratories, West Grove, PA, USA), followed by incubation for 30 minutes with an anti-rabbit HRP-Labeled Polymer (Envision kit, Dako). Peroxidase activity was revealed using diaminobenzidine (Dako). Slides were then briefly counterstained with Mayer's Hemalum solution (Merck, Darmstadt, Germany), dehydrated through a series of ethanol to xylene and mounted with DPX.

Image acquisition and analysis

Whole-mount sections were digitized using a whole-slide scanner (Leica SCN400, Leica Microsystems, Germany) and high-magnification images (20x or 40x) were captured using the Leica Image Viewer Software (Version 4.0.4). At least five pictures were taken per mouse, with 7 to 12 mice per group.

Quantification of fibrosis (% of Red stained area over total area) was performed automatically using ImageJ software (National Institutes of Health, version 1.48r).

The severity of the steatosis was scored on H&E stained liver sections based on the size and number of hepatic lipid droplets as proposed by Le Roy et al (Gut, 2013, PMID: 23197411). Scores were given as follow: 1) cells have no or a low amount of small lipid droplets (microvesicular pattern); 2) high amount of cells with a microvesicular pattern; 3) high number of cells with microvesicular pattern, mixed with cells containing large lipid droplest (macrovesicular pattern); 4) high amount of macrovesicular cells.

For inflammation, the scoring was based on the amount and density of F4/80 positive immune cells. Scores were as follow: 1) for dispersed cells in low numbers; 2) for dispersed cells in high numbers; 3) for dispersed cells in high numbers and presence of zones with dense foci; 4) for dispersed cells in higher numbers and presence of numerous infiltration foci.

Liver glycogen determination

Briefly, 30mg of powdered tissue stored at – 80°C were incubed with 200 ul of NaOH 1 M at 55°C for 1 h. Samples were mixed, neutralized with 200 ul HCl 1N, and then centrifuged at 7.0 g for 5 min at 4°C. Supernatant were removed, and 10 ul were incubated in 40 ul of a solution of amyloglucosidase 50 U/ml (Sigma) dilute in sodium acetate buffer 0.2 M (pH 7.4), while 10 ul were incubated in 40 ul of sodium acetate buffer only. The tubes were shaken for 1 h at 55°C. Then, 6 ul of each sample were deposited in 96-well plates with 200 ul of a biochemical reagent, incubated at 37°C for 10 min (Glucose God FS; Diasys). The DO was read at 505nm by spectrophotometry. The difference between conditions with amyloglucosidase and conditions with buffer only represented the glycogen content of the liver sample. Glycogen was expressed as milligrams of glucose resulting from glycogen hydrolysis per gram of tissue.

RNA extraction and real-time qPCR analysis

Total RNA was prepared from tissues using TriPure reagent (Roche). The quantification and integrity analysis of the total RNA were performed by running 1 μl of each sample on an Agilent 2100 Bioanalyzer (Agilent RNA 6000 Nano Kit, Agilent). The cDNA was prepared by reverse transcription, and real-time qPCR was performed as previously described [11]. *RPL19* was chosen as the housekeeping gene. The primers are shown in Table S6.

SDS-PAGE and immunoblotting for MyD88

To obtain total lysates, liver were homogenized with TissueLyser II (Qiagen) in RIPA buffer, and the proteins were extracted as previously described [12]. Equal amounts of proteins (20 μg) were separated by SDS-PAGE and transferred to nitrocellulose membranes. The membranes were incubated overnight at 4 °C with antibody directed against MyD88 (1:500, sc-11356, Santa Cruz Biotechnology, Inc, USA) diluted in Tris-buffered saline-Tween 20 containing 1% non-fat dry milk. The loading control was β-actin.

Bile acid analysis

The extraction and analysis of bile acids were performed according to a previous work [13]. Briefly, bile acids were extracted by protein precipitation with 10 volumes of IS-containing methanol. After the samples were vortexed and centrifuged, the supernatant was diluted 50 times in methanol:water (1:1). Bile acid separation was performed using water and acetonitrile on a Kinetex C18 column (2.1 ×100 mm with 1.7 μm particles; Phenomenex, Torrance, CA, USA). Detection was performed using a QTRAP 5500 instrument (AB Sciex, Toronto, Canada) with MRM in negative mode.

NMR spectroscopy

The total preparation time for each sample before NMR detection was less than 5 min. Mouse serum samples were stored at -80°C and thawed before use. For NMR analysis, 20 μL of serum was mixed with 2 μL of D_2O (as a field lock). In total, 20 μL of the mixture of each sample was then transferred into a 1 mm high-quality NMR capillary.

Tissue samples were prepared without thawing to minimize metabolic degradation. All the materials to be in contact with the tissue were pre-cooled to reduce tissue degradation during the sample preparation process. Frozen samples were taken from the ultra-freezer and immediately placed in a cryo-vial in liquid N_2 until insertion into a 4-mm outer diameter ZrO_2 rotor. The HR-MAS tissue sample was taken from the whole frozen specimen submerged in liquid nitrogen. The pre-cooled rotor was filled with cooled D_2O after tissue sample insertion. Cylindrical inserts were used in all cases, limiting the inner rotor volume to 50 μl. Excess D_2O was removed before rotor sealing. Tissue samples were weighted in the rotor before D_2O addition and HR-MAS measurements. Tissue fragments were weighted exclusively for sample preparation purposes. The mean sample weight was 35 ± 9 mg.

All ^{1}H NMR spectra were acquired using a standard one-dimensional pulse sequence with water suppression (Bruker Avance 600 spectrometer operating at 600.13 MHz with a 1 mm $^{1}H/^{13}C/^{15}N$ TXI probe). In total, 256 FIDs (free induction decays) were collected into 64 k data points with a spectral width of 14 ppm and a recycle delay (RD) of 1 s. The water signal was saturated with weak irradiation during the recycle delay. Before Fourier transformation, the free induction decay was multiplied by a 0.3 Hz exponential line-broadening function. Spectral chemical shift referencing the Alanine CH_3 doublet signal at 1.475 ppm was performed in all spectra. We normalized the peak intensity to the total aliphatic spectral area. Spectral regions between 0.5 and 4.5 ppm and between 5.5 and 9.5 ppm were investigated. We used available spectral databases and 2D NMR experiments to aid in the structural identification of relevant metabolites. All spectra were processed using

MestReNova (MestreLab, Santiago de Compostela, Spain) and transferred to MATLAB® (MathWorks Inc, 2006) using in-house scripts for data analysis. Signals belonging to selected metabolites were integrated by restricted spectral binning and quantified using semi-automated in-house MATLAB peak-fitting routines. These fitting routines were based on Levenburg-Marquardt optimization procedures. The target function for the optimization included experimental spectra measured for standard solutions of selected metabolites with complex multiplet patterns and theoretically generated Lorentzian-shape signals for those metabolites with simpler spectral patterns.

We used PLS_Toolbox 5.0 (Eigenvector Research, WA, USA) for MATLAB® to build the principal component analysis (PCA) and the projection latent structures discriminant analysis (PLS-DA) models. The primary advantage of PCA and PLS-DA models is that the leading sources of variability in the data are modeled by new variables that explain most of the variance in the data and, consequently, in their associated scores and loadings, allowing the visualization and understanding of different patterns and relations in the data.

PCA is able to find low dimensional embedding of multivariate data in a manner that optimally preserves the structure of the data. PCA transforms variables in a data set into a smaller number of new latent variables called principal components (PCs), which are uncorrelated to each other and which account for decreasing proportions of the total variance of the original variables. Each new PC is a linear combination of the original variation such that a compact description of the variation within the data set is generated. Observations are assigned scores according to the variation measured by the principal component with those having similar scores being clustered together.

PLS-DA is a classification technique that encompasses the properties of partial least squares regression with the power of discriminant analysis [14]. From a mathematical point of view, PLS-DA is a supervised extension of PCA used to distinguish two or more classes by

searching for variables (X matrix) that are correlated to class membership (Y matrix). In this approach, the axes are calculated to maximize class separation and can be used to examine separation that would otherwise be across three or more principal components.

The PLS-DA models were cross-validated by the leave-one-out method. Cross validation is a very useful tool that provides two critical functions in chemometrics. First, cross validation enables an assessment of the optimal complexity of a model. Second, cross validation allows an estimation of the performance of a model when it is applied to unknown data. For a given data set, cross validation involves a series of experiments, hereby called sub-validation experiments, each of which involves the removal of a subset of individuals from a dataset, construction of a model using the remaining objects in the dataset, and subsequent application of the resulting model to the removed objects. Therefore, each sub-validation experiment involves testing a model with objects that were not used to build the model. Typical cross validation involves more than one sub-validation experiment by selecting different subsets of individuals for model building and testing. Leave-one-out cross validation involves the use of a single observation from the original sample as the validation data and the remaining observations as the training data. This process is repeated in a manner that each observation in the sample is used once as the validation data. The leave-one-out method is ideally suited for datasets with a limited number of samples.

Study population, liver histology and patient classification:

A cohort study included morbidly obese patients undergoing bariatric surgery as previously described [15]. In short: a liver biopsy was performed using a 16G trucut biopsy needle for histopathological assessment and from which RNA was extracted. Histological scoring was performed by expert liver pathologists blinded to all clinical information. Features of NASH were semi-quantitatively scored according to the NASH-Clinical Research Network Scoring

System criteria [16]. Patients with proven cirrhosis or cases with borderline features of NASH were excluded for further analysis. We subsequently classified the patients into 3 distinct groups according their liver histology: Group 1 (OBESE CONTROL): patients with < 5% steatosis, NAS score for all patients in this group is 0; Group 2 (NAFL): NAFLD without evidence of inflammation or NASH, NAS score < 4, Group 3 (NASH): NASH without significant fibrosis, NAS score ≥ 5 and fibrosis score 0-1. All patients gave written informed consent and the study protocol was approved by the research institution ethical committee (KUL).

RNA-extraction, cDNA synthesis and Quantitative RT-PCR:

Liver tissue was homogenized with Trizol (Invitrogen Life Technologies, USA) and RNA isolated by means of RNeasy Kit (Qiagen, Chatsworth, CA). RNA quality and quantity was determined by NanoDrop spectrophotometer (NanoDrop Technologies, Centreville, DE) and Agilent 2100 BioAnalyzer (Agilent, Palo Alto, CA) respectively.

Microarray and Data Processing

A total of 100 ng per sample of total RNA spiked with bacterial RNA transcript-positive controls (Affymetrix) was amplified and labeled using the GeneChip 3' IVT express kit (Affymetrix). All steps were performed according to the manufacturer's protocol (Affymetrix). To assess the raw probe signal intensities, chips were scanned using a GeneChip scanner 3000 (Affymetrix). Analysis of the microarray data was performed in the R programming environment, in conjunction with the packages developed within the Bioconductor project [17]. The analysis was based on the RMA expression levels of the probe sets, computed with the package xps (version 1.16.0). Differential expression was assessed via the moderated t-statistic, described by Smyth et al, [18, 19] and implemented in the limma package (version 3.12.1). To control the false-discovery rate, multiple testing corrections were performed using the Benjamini-Hochberg's method [20].

Data are available through National Center for Biotechnology Information (GSE59045).

Supplemental References

1 Essaghir A, Dif N, Marbehant CY, Coffer PJ, Demoulin JB. The transcription of FOXO genes is stimulated by FOXO3 and repressed by growth factors. The Journal of biological chemistry 2009;284:10334-42.

2 Huang da W, Sherman BT, Lempicki RA. Systematic and integrative analysis of large gene lists using DAVID bioinformatics resources. Nature protocols 2009;4:44-57.

3 Essaghir A, Toffalini F, Knoops L, Kallin A, van Helden J, Demoulin JB. Transcription factor regulation can be accurately predicted from the presence of target gene signatures in microarray gene expression data. Nucleic acids research 2010;38:e120.

4 Everard A, Matamoros S, Geurts L, Delzenne NM, Cani PD. Saccharomyces boulardii Administration Changes Gut Microbiota and Reduces Hepatic Steatosis, Low-Grade Inflammation, and Fat Mass in Obese and Type 2 Diabetic db/db Mice. mBio 2014;5.

5 DeSantis TZ, Hugenholtz P, Larsen N, Rojas M, Brodie EL, Keller K, *et al.* Greengenes, a chimera-checked 16S rRNA gene database and workbench compatible with ARB. Appl Environ Microbiol 2006;72:5069-72.

6 McDonald D, Price MN, Goodrich J, Nawrocki EP, DeSantis TZ, Probst A, *et al.* An improved Greengenes taxonomy with explicit ranks for ecological and evolutionary analyses of bacteria and archaea. The ISME journal 2012;6:610-8.

7 Everard A, Geurts L, Caesar R, Van Hul M, Matamoros S, Duparc T, *et al.* Intestinal epithelial MyD88 is a sensor switching host metabolism towards obesity according to nutritional status. Nature communications 2014;5:5648.

8 Geurts L, Everard A, Van Hul M, Essaghir A, Duparc T, Matamoros S, *et al.* Adipose tissue NAPE-PLD controls fat mass development by altering the browning process and gut microbiota. Nature communications 2015;6:6495.

9 Folch J, Lees M, Sloane Stanley GH. A simple method for the isolation and purification of total lipides from animal tissues. JBiolChem 1957;226:497-509.

10 Geurts L, Everard A, le Ruyet P, Delzenne NM, Cani PD. Ripened dairy products differentially affect hepatic lipid content and adipose tissue oxidative stress markers in obese and type 2 diabetic mice. J Agric Food Chem 2012;60:2063-8.

11 Everard A, Lazarevic V, Gaia N, Johansson M, Stahlman M, Backhed F, *et al.* Microbiome of prebiotic-treated mice reveals novel targets involved in host response during obesity. The ISME journal 2014;8:2116-30.

12 Pachikian BD, Essaghir A, Demoulin JB, Neyrinck AM, Catry E, de Backer FC, *et al.* Hepatic n-3 polyunsaturated fatty acid depletion promotes steatosis and insulin resistance in mice: genomic analysis of cellular targets. PLoSONE 2011;6:e23365.

13 Tremaroli V, Karlsson F, Werling M, Stahlman M, Kovatcheva-Datchary P, Olbers T, *et al.* Roux-en-Y Gastric Bypass and Vertical Banded Gastroplasty Induce Long-Term Changes on the Human Gut Microbiome Contributing to Fat Mass Regulation. Cell Metab 2015;22:228-38.
14 Trygg J, Holmes E, Lundstedt T. Chemometrics in metabonomics. Journal of proteome research 2007;6:469-79.
15 du Plessis J, van Pelt J, Korf H, Mathieu C, van der Schueren B, Lannoo M, *et al.* Association of Adipose Tissue Inflammation With Histologic Severity of Nonalcoholic Fatty Liver Disease. Gastroenterology 2015;149:635-48 e14.
16 Brunt EM, Kleiner DE, Wilson LA, Belt P, Neuschwander-Tetri BA, Network NCR. Nonalcoholic fatty liver disease (NAFLD) activity score and the histopathologic diagnosis in NAFLD: distinct clinicopathologic meanings. Hepatology 2011;53:810-20.
17 Gentleman RC, Carey VJ, Bates DM, Bolstad B, Dettling M, Dudoit S, *et al.* Bioconductor: open software development for computational biology and bioinformatics. Genome Biol 2004;5:R80.
18 Smyth GK. Linear models and empirical bayes methods for assessing differential expression in microarray experiments. Stat Appl Genet Mol Biol 2004;3:Article3.
19 Smyth GK, Michaud J, Scott HS. Use of within-array replicate spots for assessing differential expression in microarray experiments. Bioinformatics 2005;21:2067-75.
20 Benjamini Y, Hochberg, Y. Controlling the false discovery rate: a practical and powerful approach to multiple testing. Journal of the Royal Statistical Society Series B (Methodological) 1995;57:289-300.